Article

Unexpected subcellular distribution of a specific isoform of the Coxsackie and adenovirus receptor, CAR-SIV, in human pancreatic beta cells

Ese Ifie[1], Mark A. Russell[1], Shalinee Dhayal[1], Pia Leete[1], Guido Sebastiani[2], Laura Nigi[2], Francesco Dotta[2], Varpu Marjomäki[3], Decio L. Eizirik[4], Noel G. Morgan[1], Sarah J. Richardson[1]

[1]Islet Biology Exeter (IBEx), Institute of Biomedical and Clinical Sciences, University of Exeter Medical School, RILD Building (Level 4), Barrack Road, Exeter, EX2 5DW, UK

[2]Department of Medicine, Surgery and Neurosciences, University of Siena and Fondazione Umberto Di Mario ONLUS—Toscana Life Sciences, Siena Italy

[3]Department of Biological and Environmental Science/Nanoscience Center, University of Jyväskylä, Jyväskylä, Finland

[4]Université Libre de Bruxelles (ULB) Center for Diabetes Research and Welbio, Medical Faculty, Université Libre de Bruxelles, Brussels, Belgium

Corresponding author: S. Richardson, Islet Biology Exeter (IBEx), Institute of Biomedical and Clinical Sciences, University of Exeter Medical School, RILD Building (Level 4), Barrack Road, Exeter, EX2 5DW, UK

email: s.richardson@exeter.ac.uk;

Tweet: Does the CAR help steer the way for insulin secretion?

Received: 6 December 2017 / Accepted: 2 July 018

Abstract

Aims/hypothesis The Coxsackie and adenovirus receptor (CAR) is a transmembrane cell-adhesion protein that serves as an entry receptor for enteroviruses and may be essential for their ability to infect cells. Since enteroviral infection of beta-cells has been implicated as a factor that could contribute to the development of type 1 diabetes, it is often assumed that CAR is displayed on the surface of human beta cells. However, CAR exists as multiple isoforms and it is not known whether all isoforms subserve similar physiological functions. In the present study, we have determined the profile of CAR isoforms present in human beta cells and monitored the subcellular localisation of the principal isoform within the cells.

Methods Formalin-fixed, paraffin-embedded pancreatic sections from non-diabetic individuals and those with type 1 diabetes were studied. Immunohistochemistry, confocal immunofluorescence, electron microscopy and western blotting with isoform-specific antisera were employed to examine the expression and cellular localisation of the five known CAR isoforms. Isoform-specific qRT-PCR and RNA sequencing (RNAseq) were performed on RNA extracted from isolated human islets.

Results An isoform of CAR with a terminal SIV motif and a unique PDZ-binding domain was expressed at high levels in human beta cells at the protein level. A second isoform, CAR-TVV, was also present. Both forms were readily detected by qRT-PCR and RNAseq analysis in isolated human islets. Immunocytochemical studies indicated that CAR-SIV was the principal isoform in islets and was localised mainly within the cytoplasm of beta-cells, rather than at the plasma membrane. Within the cells it displayed a punctate pattern of immunolabelling, consistent with its retention within a specific membrane-bound compartment. Co-immunofluorescence analysis revealed significant co-localisation of CAR-SIV with zinc transporter protein 8 (ZnT8), prohormone convertase 1/3 (PC1/3) and insulin, but not

proinsulin. This suggests that CAR-SIV may be resident mainly in the membranes of insulin secretory granules. Immunogold labelling and electron microscopic analysis confirmed that CAR-SIV was localised to dense-core (insulin) secretory granules in human islets, whereas no immunolabelling of the protein was detected on the secretory granules of adjacent exocrine cells. Importantly, CAR-SIV was also found to co-localise with protein interacting with C-kinase 1 (PICK1), a protein recently demonstrated to play a role in insulin granule maturation and trafficking.

Conclusions/interpretation: The SIV isoform of CAR is abundant in human beta cells and is localised mainly to insulin secretory granules, implying that it may be involved in granule trafficking and maturation. We propose that this subcellular localisation of CAR-SIV contributes to the unique sensitivity of human beta cells to enteroviral infection.

KEYWORDS

Beta cells; Coxsackie and adenovirus receptor; Coxsackievirus B; Enterovirus; Insulin granule; Pancreas; Protein interacting with C-kinase 1 (PICK1)

Abbreviations

CAR	Coxsackie and adenovirus receptor
CAR-CT	Coxsackie and adenovirus receptor C-terminus
CVB	Coxsackievirus B
ECD	Extracellular domain
FFPE	Formalin-fixed, paraffin–embedded
GAPDH	Glyceraldehyde 3-phosphate dehydrogenase
LCM	Laser capture microdissected
MCC	Manders co-localisation coefficient

PC1/3	Prohormone convertase 1/3
PICK1	Protein interacting with C-kinase 1
RNAseq	RNA sequencing
ZnT8	Zinc transporter protein 8

Research in context

What is already known about this subject?

- Human pancreatic beta cells are susceptible to infection by enteroviruses, including Coxsackievirus B, which use the Coxsackie and adenovirus receptor (CAR) as their entry receptor
- CAR exists as at least five structurally distinct isoforms, which vary in their subcellular localisation and ability to mediate infection

What is the key question?

- Which CAR isoforms are expressed in the human pancreas?

What are the new findings?

- Human pancreatic beta cells principally express a specific isoform of CAR (CAR-SIV) that is localised to insulin secretory granules within the beta cells
- CAR-SIV co-localises with protein interacting with C-kinase 1 (PICK1), a protein involved in insulin granule maturation and trafficking, suggesting a previously unrecognised role for CAR-SIV in this process
- The localisation of CAR-SIV within the insulin secretory granules may contribute to the unique sensitivity of human beta cells to enteroviral infection

How might this impact on clinical practice in the foreseeable future?

- These studies suggest that CAR could be targeted selectively in beta cells as a means of minimising enteroviral infection and the development of islet autoimmunity

Introduction

Epidemiological and pathological studies have linked enteroviral infections with the development of type 1 diabetes mellitus [1], but the mechanisms by which this might promote islet autoimmunity remain uncertain. One possibility is that islet cells are particularly sensitive to infection by enteroviruses and, in accord with this, enterovirus serotypes that are most often associated with type 1 diabetes (e.g. Coxsackievirus B [CVB]) have a clear tropism for human beta cells [2-4]. Additional support comes from evidence that enterovirus proteins are present in the beta cells of individuals with type 1 diabetes [5, 6] and that specific viral response pathways are activated in such cells [7, 8].

In order for enteroviruses to infect cells, they must bind to specific cell surface proteins that serve as vehicles to mediate their entry. Such binding is thought to alter the conformation of the viral capsid to facilitate the entry of viral RNA into the target cell. An endogenous cellular protein known as the Coxsackie and adenovirus receptor (CAR) is one such viral receptor. CAR is a transmembrane protein involved in homotypic cell adhesion and tight junctional integrity [9] but also serves as a primary cellular attachment protein for CVBs and adenoviruses [10], presumably in a subversion of its normal physiological role.

Full-length CAR is encoded by the *CXADR* gene, which comprises eight exons and yields a protein with an extracellular domain (ECD) linked by a single transmembrane region to a cytoplasmic tail. Differential splicing yields at least five different isoforms (Fig. 1a,b), but only two of these contain the transmembrane domain and are likely to be retained within cells. Structural studies have suggested that enteroviruses bind to the D1 domain in the extracellular region of the protein [11, 12] and, accordingly, four of the isoforms (designated CAR-SIV, CAR-TVV, CAR4/7 and CAR3/7) have been shown to bind enterovirus. However, only CAR-SIV and CAR-TVV retain the transmembrane domain and are thus able to mediate a productive

infection in cells. The two soluble isoforms are released from cells and may protect from infection by sequestering active virus in the extracellular fluid [11].

Interestingly, the two isoforms bearing a transmembrane domain vary only in the sequence of the final 26 (CAR-SIV) or 13 (CAR-TVV) amino acids, but are differentially localised within cells and may fulfil different functions [13]. The CAR-SIV isoform (also known as CAR^{Ex7}[13]) is encoded by the first seven exons of the human *CXADR* gene and is expressed preferentially on the basolateral surface of polarised cells. In contrast, the C-terminal region of the CAR-TVV isoform (also known as CAR^{Ex8}) is produced from a cryptic splice site within the seventh exon linked to exon 8, and is expressed apically [13]. The C-terminal region encodes a consensus PDZ-binding domain whose amino acid sequence varies between the CAR-SIV and the CAR-TVV forms, which probably accounts for the differential localisation of the two variants within polarised cells [13-16]. In support of this, both the SIV and TVV forms of CAR can interact with proteins such as membrane-associated guanylate kinase, WW and PDZ domain-containing protein 1b (MAGI-Ib), postsynaptic density protein 95 (PSD-95) [13, 15, 16] and zonula occludens-1 (ZO-1) [14], but only the CAR-SIV isoform interacts with protein interacting with C-kinase 1 (PICK1) [13]. Strikingly, PICK1 is abundantly expressed in beta cells and has recently been shown to control insulin granule trafficking. Indeed, loss of PICK1 results in impaired glucose tolerance and reduced serum insulin concentrations in experimental animals [17, 18]. Thus, an interaction between PICK1 and the SIV isoform of CAR in beta cells could be of functional importance.

To date, few studies have examined the expression and distribution of CAR isoforms in human beta cells [3, 19]. Ylipaasto et al [3] confirmed a role for CAR by demonstrating that pre-treatment of isolated human islets with a blocking antibody (clone RmcB) protected the cells from CVB infection [3]. More recently, CAR expression was confirmed in human pancreas, albeit using an antiserum that does not discriminate between the various isoforms [20]. We

have thus characterised and mapped the expression and distribution of CAR isoforms in human pancreas.

Methods

Tissue and cell lines Formalin-fixed, paraffin–embedded (FFPE) pancreatic sections from the Exeter Archival Diabetes Biobank (http://foulis.vub.ac.be/) and from the Network for Pancreatic Organ donors with Diabetes (nPOD) (Florida, USA) were studied. Samples were from 21 non-diabetic individuals (age range 4-47 years) and ten individuals with type 1 diabetes (age range 6-47 years; see electronic supplementary material [ESM] Table 1). Isolated human islets were obtained from the Oxford Centre for Islet Transplantation (Oxford, UK) or purchased from Lonza (Basel, Switzerland). On arrival, islets were cultured for 24h at 37°C and then fixed and processed for immunostaining by standard immunofluorescence (FFPE) techniques, or stored at −80^{o}C for RNA extraction. Ethics approval (West of Scotland Research Committee 4 (WoSREC4); 15/WS/0258) was gained for all the samples studied. The pancreatic tissue samples from the Exeter Archival Diabetes Biobank and nPOD were selected based on age of demise, and in the case of Type 1 diabetes, duration of disease; tissue quality; sample availability (which is restricted within these biobanks) and appropriateness of tissue for IHC/ IF approaches. Samples with extensive autolysis or evidence of other unrelated pancreatic diseases were excluded. Blinding of donor type and immunofluorescence stain was performed for the co-localisation studies. The human beta cell lines EndoC-βH1 and 1.1B4s were cultured as described in ESM Methods.

Antibodies Three different anti-CAR sera were employed (ESM Table 2) based on their selective immunoreactivity against the C-terminus (CAR-CT) or regions within the ECD

(CAR-ECD and CAR-RmcB) of the protein, respectively, and validated as described below and in ESM Fig. 1. These allowed the various isoforms of CAR to be distinguished, as illustrated in Fig. 1b. All other antisera are described in ESM Table 2.

Mutagenesis Site-directed mutagenesis was performed to remove the final three amino acids (SIV) of CAR-SIV to examine the specificity of the CAR-CT antiserum (ESM Methods).

Western blotting The production of CAR in human islets and EndoC-βH1 cells and the specificity of the CAR-CT and CAR-RmcB antisera were assessed using western blotting (ESM Methods).

Flow cytometry The specificity of the CAR-CT and CAR-RmcB antisera was assessed using flow cytometry (ESM Methods).

Immunohistochemistry This was performed using a standard immunoperoxidase approach [21]. Bright-field image acquisition was performed using a Nikon 50i Microscope fitted with a DS-Fi camera and a DSL2 camera control unit (Nikon, Kingston Upon Thames, UK). Antibody details and conditions are described in ESM Table 2.

Immunofluorescence (FFPE) To examine multiple antigens within the same section, samples were probed in a sequential manner with up to three different antibodies (ESM Table 2) [22]. Pancreas sections were initially subjected to heat-induced epitope retrieval in 10mmol/l citrate buffer (pH 6), and relevant antigen–antibody complexes were detected using secondary antibodies conjugated with fluorescent dyes (Alexa Fluor anti-mouse 488, anti-rabbit 555, and anti-guinea pig 568 or 647; Invitrogen, Paisley, UK). Cell nuclei were stained with DAPI. After

mounting, images were captured either with a Leica AF6000 microscope (Leica, Milton Keynes, UK), then were processed using the standard LAS X Leica software platform (Version 3.3.0.16799), or with a Leica SP8 confocal microscope and Hyvolution2 deconvolution software (Scientific Volume Imaging, Hilversum, The Netherlands). Co-localisation analysis was undertaken with a JACoP plugin from Image J, version 1.48 Java 1.6.0 _20 (https://imagej.nih.gov/ij/plugins/track/jacop2.html).

Quantitative RT-PCR (qRT-PCR)/semi-quantitative RT-PCR The relative expression levels of the CAR-SIV, CAR-TVV, CAR4/7, CAR3/7 and CAR2/7 isoforms in isolated human islets and laser capture microdissected (LCM) islets were determined using qRT-PCR (ESM Methods).

RNAseq RNA sequencing (RNAseq) was performed using islets obtained from normoglycaemic human islet donors or EndoC-βH1 cells as previously described [23]. Genes and transcripts were assigned a relative coverage rate as measured in reads per kilobase of exon model per million mapped reads and compared with 15 other normal human tissues, analysed by RNAseq and deposited at the Illumina BodyMap 2.0 dataset (GEO accession number GSE30611), accessed on August 9, 2017.

Cryoimmune electron microscopy We used cryoimmune electron microscopy to assess and quantify the localisation of CAR-SIV, zinc transporter protein 8 (ZnT8), insulin and proinsulin in human pancreas samples as described previously [24] and in the ESM Methods.

Co-immunoprecipitation of PICK1 with CAR This was performed in EndoC-βH1 cells and human islets as described in ESM Methods.

Statistical analysis Immunofluorescence images of islets were selected randomly from stained pancreas sections. The Pearson correlation coefficient was used to estimate the co-localisation between proteins using the JACoP plugin from Image J. Values for the Pearson correlation coefficient ranged from 0 for no correlation, to 1 for a positive correlation. GraphPad Prism 5.04 (La Jolla, California, USA) was employed for all statistical analysis, and data are expressed as means ±SEM. Statistical significance was calculated using one-way ANOVA, and the Bonferroni multiple comparison test was used for multiple comparisons. A p value <0.05 was considered statistically significant.

Results

Differential CAR immunostaining in human pancreas The availability of antisera directed against different regions of the CAR protein (Fig. 1b) enabled the expression profiles of the two isoforms bearing a transmembrane domain to be studied. The antiserum designated CAR-CT was raised against a peptide containing the C-terminal 35 amino acids of the CAR-SIV protein and required the presence of the triplet ‘’SIV’ sequence at the immediate C-terminus for immunoreactivity. As such, it did not label any other isoform of CAR. This specificity was confirmed by transfection of 1.1B4 cells with constructs encoding either the full-length CAR-SIV or a variant in which the final three amino acids (SIV) had been removed by targeted mutagenesis (ESM Methods). Western blotting and immunofluorescence staining confirmed immunorecognition of the full-length CAR-SIV isoform, but not the truncated form, by the CAR-CT antiserum (ESM Fig. 1).

Two further CAR antibodies, CAR-ECD (Abcam, Cambridge, UK) and RmcB (Merck Millipore, Watford, UK), both of which recognise the ECD of human CAR, were also used. By deploying a panel of approaches (western blotting, immunofluorescence staining of fixed cells, flow cytometry and immunohistochemistry in FFPE sections), it was found that the CAR-ECD antiserum worked effectively in both western blotting and immunohistochemistry, whereas the RmcB clone was most suitable for immunofluorescence staining of fixed cells or flow cytometry. As noted above, both the CAR-ECD and RmcB antibodies recognise multiple isoforms of CAR including CAR-SIV, CAR-TVV and CAR4/7 (ESM Fig. 1b,c).

Use of these differentially specific antisera revealed that various isoforms of CAR are expressed differentially among the exocrine and endocrine compartments of the human pancreas (Fig. 1c,d). Importantly, the CAR-CT antiserum labelled only islet cells (Fig. 1c) whereas use of the CAR-ECD antiserum resulted in labelling of both exocrine and endocrine tissue (Fig. 1d). An identical staining pattern was confirmed in a total of eight pancreases from non-diabetic donors (within the Exeter and nPOD Biobanks), ranging in age from 4 weeks to 59 years of age (ESM Table 1).

Confirmation of SIV isoform expression by qRT-PCR in human islets Isoform-specific primers were used to analyse *CXADR* isoform expression (ESM Table 3) by qRT-PCR in RNA extracted from isolated human islets (ESM Table 4). This revealed that transcripts encoding the CAR-SIV and CAR-TVV isoforms were expressed at the highest levels, while the soluble CAR4/7 isoform was less abundant (Fig. 2a). The two shorter isoforms CAR3/7 and CAR2/7 were barely detectable. These results were confirmed in a second set of independent samples in which RNA was isolated from LCM islets (Fig. 2b; ESM Table 5). This was further confirmed by RNAseq analysis of isolated human islets (Fig. 2c). Importantly, CAR-SIV was enriched threefold compared with CAR-TVV in the human pancreatic beta cell line EndoC-

βH1 (ESM Fig. 2a; ESM Methods) [25], and semi-quantitative RT-PCR analysis of RNA extracted from two highly purified preparations of human islets revealed that the expression of CAR-SIV was greater than that of CAR-TVV (ESM Fig. 2b). Finally, the presence of the SIV isoform was verified by western blotting in isolated human islets and EndoC-βH1 cell using the CAR-CT and CAR-ECD antisera (Fig. 2d).

The SIV isoform is expressed preferentially in human beta cells To determine whether the SIV isoform of CAR is preferentially localised to a specific endocrine cell subset, combined immunofluorescence staining using anti-CAR-CT, insulin and glucagon was performed. This revealed that expression of the CAR-SIV isoform was restricted solely to beta cells in human pancreas sections (Fig. 3a) and isolated human islets (Fig. 3b). Somewhat surprisingly, rather than being localised to the cell surface, the CAR-SIV isoform was distributed mainly within the cytoplasm of beta cells. Confocal microscopy revealed that CAR-SIV displayed a punctate distribution and that it specifically co-localised with insulin, suggesting a possible association with secretory granules (Fig. 3c). A similar pattern of punctate immuno-co-localisation with insulin was observed when using an alternative CAR antiserum (CAR-ECD; data not shown). To explore these relationships further, the expression of CAR-SIV was investigated in the pancreases of a series of people with type 1 diabetes (ten individuals; 3-42 years of age; ESM Table 1, ESM Fig. 3) and islet autoantibody-positive non-diabetic individuals (two participants, aged 18 and 37 years, respectively). The samples from individuals with type 1 diabetes contained both insulin-deficient islets and insulin-containing islets. CAR-SIV expression was absent from the insulin-deficient islets, but was clearly visible in residual insulin-containing islets. Neither the subcellular distribution nor the staining intensity differed between the type 1 diabetic, autoantibody-positive non-diabetic and non-diabetic islets (ESM Fig. 3 and data not shown). Finally, by applying the CAR-CT antibody to a human tissue microarray (gift from

Alan Foulis; University of Glasgow, UK), it was confirmed that the SIV isoform could be variously found at the surface membrane (testes and bladder small cell carcinoma) and/or in cytoplasmic regions (stomach and islets) within normal and cancerous tissues (ESM Fig. 4). RNAseq data supported this expression profile (ESM Fig. 4).

CAR-SIV co-localises with secretory granule proteins in beta cells In order to verify the localisation of CAR-SIV in beta cells, confocal co-immunofluorescence studies were performed to localise certain other proteins (ZnT8, Fig 4a; prohormone convertase 1/3 [PC1/3], Fig 4b; and proinsulin, Fig 4c) known to be present in secretory granules. Calculation of the Pearson correlation coefficient confirmed that insulin strongly associated with ZnT8 (0.94±0.01; Fig. 4d). Importantly, CAR-SIV also correlated strongly with insulin (0.95±0.02; Fig. 4d) and PC1/3 (0.81±0.02; Fig. 4d). In contrast, CAR-SIV did not associate with glucagon (0.05±0.02; Fig. 4d,e) and was more weakly associated with proinsulin (0.55±0.04; Fig 4d). High-resolution confocal microscopy confirmed the co-localisation of CAR-SIV with ZnT8 (Fig. 4f) and PC1/3 (Fig. 4g), and showed that CAR-SIV and proinsulin were less frequently co-localised (Fig. 4h). Using a more sophisticated reciprocal analysis, it was confirmed that the majority of CAR-SIV co-localised with insulin (Manders co-localisation coefficient [MCC] 0.914±0.016) and that this was also true in reverse (i.e. the proportion of insulin co-localising with CAR-SIV was high (MCC 0.912±0.028; ESM Fig. 5).

By contrast, although a large proportion of total proinsulin co-localised with CAR-SIV (MCC 0.708±0.082), this did not hold in reverse (CAR-SIV:proinsulin, MCC 0.211±0.042) because little proinsulin escaped into mature secretory granules. Together, these findings suggest that CAR-SIV is present in both immature and mature insulin secretory granules in human beta cells.

Cryoimmune electron microscopy confirms that CAR-SIV is localised to insulin secretory granules To confirm more directly that the CAR-SIV isoform localises to insulin secretory granules, immunogold labelling was performed on thin frozen sections using the post-embedding Tokuyasu method [24] with antisera against CAR-SIV (10 nm gold particles) and ZnT8 (5 nm gold particles). This revealed that both antisera localise to secretory granules in human pancreas sections (Fig. 5); the characteristic electron-dense appearance of the granule cores implies that they contain insulin. This was verified by immunostaining with anti-insulin (ESM Fig. 6). By contrast, gold particles were not concentrated in the secretory granules of exocrine cells. Immunogold labelling of insulin secretory granules with the CAR-CT antibody demonstrated that localisation was least abundant in the centre of the granule cores and preferentially displayed at their periphery (Fig. 5c,d). Labelling of ZnT8 showed a similar distribution.

Quantification of 841 CAR-SIV immunogold particles from 21 different micrographs, across 1291 different membrane intersections, revealed that CAR-SIV was most abundant on mature insulin secretory granules (79%). CAR-SIV was also observed in immature insulin granules (14.4%), but was rarely observed in beta cell nuclei (2.5%), mitochondria (1.0%) or endoplasmic reticulum (1.1%) or on the plasma membrane (1.2%; Fig. 5b,e). Of note, uranyl acetate yields a ‘negative contrast’ for organelle membranes in the staining method employed, and as a consequence the appearance of the secretory granules differs from that seen with osmium labelling.

To further confirm the presence of CAR-SIV in the insulin granules at different stages of granule maturation, immunogold labelling of normal pancreas sections to detect proinsulin (20 nm gold particles), CAR-SIV (10 nm gold particles) and insulin (5 nm gold particles) was performed (ESM Fig 6). This revealed the presence of CAR-SIV in immature granules, defined as proinsulin and CAR-SIV positive (ESM Fig. 6c); maturing granules, defined as proinsulin,

insulin and CAR-SIV positive (ESM Fig. 6d); and mature granules, defined as insulin and CAR-SIV positive (ESM Fig. 6e). Examination of 122 granules containing CAR-SIV revealed that six (4.9%) were also positive for proinsulin (immature granules); 30 (24.6%) were also positive for proinsulin and insulin (maturing granules), and the majority 86 (70.5%) were positive for insulin (mature granules). Taken together, these results suggest that CAR-SIV is present within the granule membrane at all stages of granule maturation.

CAR-SIV co-localises with PICK1 in insulin secretory granules PICK1 may play an important role in insulin granule trafficking and maturation [18], and the SIV isoform of CAR, but not the TVV isoform, selectively interacts with PICK1 in other cell types [13, 15]. To assess whether CAR-SIV co-localises with PICK1 in human beta cells, further confocal co-immunofluorescence studies (Fig. 6) and immunoprecipitation (ESM Fig. 7) studies were performed. PICK1 was readily detected in islet endocrine cells (in both beta and non-beta cells; Fig. 6a) and, importantly, it co-localised with CAR-SIV in beta cells (Fig. 6a) and was co-immunoprecipitated with CAR from EndoC-βH1 cells and human islets (ESM Fig. 7). Pearson's correlation analysis of the immunofluorescence signals (Fig. 6b) confirmed a strong association between PICK1 and both CAR-SIV (0.73±0.02) and insulin (0.84±0.04).

To examine the co-localisation of PICK1, CAR-SIV and insulin in more detail, confocal microscopy coupled with Hyvolution software was employed to provide improved resolution. This confirmed the intimate association between PICK1 and the SIV isoform of CAR within insulin secretory granules (Fig. 6c). PICK1 was also observed in association with the secretory granules of other islet non-beta endocrine cells, but CAR-SIV was not detected in those cells (Fig. 6).

Discussion

The present study reveals that the SIV isoform of CAR is expressed selectively by beta cells in the human pancreas. This finding was confirmed at both the RNA and protein levels. We also discovered that the subcellular localisation of CAR-SIV was atypical: the protein was found mainly within the cytoplasmic domain of beta cells rather than at the cell surface.

We used both immunological and molecular biological approaches to investigate CAR expression in human islet cells, and the results were concordant. Thus, analysis of RNA extracted either from isolated human islets or laser capture microdissected islets revealed that two major isoforms of CAR, CAR-SIV and CAR-TVV, were present. Both of these contain a single transmembrane domain, implying that they could each be localised within defined, membrane-limited, compartments in the islet cells, as in other cell types [13]. The results favoured a preponderance of the CAR-SIV isoform in islets, and immunohistochemical analysis confirmed abundant production of CAR-SIV protein in human islet cells, contrasting with its absence from the exocrine pancreas. Taken as a whole, the results suggest that the major isoform of CAR present in human islets is CAR-SIV, although CAR-TVV is also present. CAR-SIV is expressed preferentially in beta cells, since we were unable to find evidence for its expression in ‘non-beta’ islet cells. By contrast, use of less selective antisera suggested that additional isoforms of CAR (including CAR-TVV) may be present among the other non-beta endocrine cells. This would be consistent with the analysis of RNA expression.

The primary subcellular localisation of CAR in beta cells has not been extensively addressed in previous work [3, 20] but, despite this, in other cell types a consensus has emerged that this protein is often localised within tight junctional complexes at the plasma membrane [13, 14, 26]. As such, CAR would be expected to be present at the cell surface, where it could fulfil a secondary (presumably subverted) role as a vehicle for viral entry. Thus, the present

demonstration that CAR-SIV is present in human beta cells is consistent with the known sensitivity of these cells to infection by various enterovirus serotypes. However, the intriguing discovery that this isoform was localised primarily at an intracellular site in beta cells suggests a more complex scenario (and a different physiological role) compared with other cells in which CAR resides mainly on the plasma membrane.

High-resolution confocal microscopic analysis was used to examine in more detail the unexpected subcellular localisation of CAR-SIV in beta cells. This revealed a punctate, cytoplasmic immunolabelling pattern for CAR-SIV, consistent with its distribution in a distinct intracellular organelle compartment. Additional studies demonstrated that this immunolabelling profile correlated with that of insulin, as well as with two additional secretory granule proteins, ZnT8 and PC1/3, thereby implying a localisation within beta cell insulin secretory granules. Direct confirmation of this was provided by cryoimmune electron microscopy studies in which immunogold methods allowed the visualisation of CAR-SIV, principally in association with the dense-core granules characteristically found in beta cells. By contrast, no labelling was seen in the equivalent secretory granules found in adjacent exocrine cells, implying that CAR-SIV is not absolutely required for secretory granule biogenesis in all cell types.

Importantly, and consistent with results obtained in other cells [18], we also noted that CAR-SIV co-localised with, and could be immunoprecipitated with, the PDZ domain protein PICK1 in beta cells. PICK1 plays a specific role in insulin secretory granule maturation [18, 27], and it is conceivable that CAR-SIV serves as a selective binding partner for PICK1 in beta cells, thereby concentrating the two proteins within maturing secretory granules. Consistent with this hypothesis, we found by immunofluorescence analysisat the SIV isoform of CAR is much more strongly associated with mature insulin than with proinsulin, suggesting that CAR (and PICK1)

may become concentrated in secretory granules as these mature beyond their emergence from the *trans*-Golgi network.

If this model is correct, it has additional important consequences. In particular, the model predicts that the C-terminus of CAR-SIV must face the extragranular environment, since its PDZ-binding domain is located in this region and would only be available to interact with cytoplasmic PICK1 (or other cytoplasmic PDZ-binding proteins) in this orientation. As such, the putative ECD of CAR-SIV would then face the lumen of the granule, with the single transmembrane region serving to anchor the protein in this orientation in the limiting membrane surrounding the granule. Thus, the region of SIV required for the binding of enteroviruses would face the interior of the secretory granule during maturation. It follows from this that the ECD of CAR-SIV would become displayed on the external face of the plasma membrane following the fusion of the secretory granule and plasma membranes during exocytosis.

These considerations are summarised in Fig. 7 and suggest that enteroviral entry into beta cells may be facilitated under conditions in which the rate of secretory granule exocytosis is high (and granule membrane recycling rates are correspondingly elevated). Thus, CAR-SIV appears to be configured in beta cells such that it can interact with PDZ-binding proteins during secretory granule maturation, and its virus-binding domain becomes exposed to the extracellular environment during exocytosis. Of note, most of the autoantigens in type 1 diabetes are expressed in the insulin granule [28] and the preferential localisation of viral receptors in the granule indicates a potential mechanism by which CVB infection may modify the processing of granule proteins, to promote the generation of autoantigens.

In support of our conclusions, Ylipaasto et al [3] demonstrated that the pre-treatment of human islets with a blocking antibody directed solely against externally oriented CAR attenuated infection with Coxsackie viruses. When coupled with our finding that the majority of CAR is located intracellularly in islet cells, this suggests that externalisation of the protein occurs to

mediate viral entry. Moreover, we also note Hodik et al's [29] demonstration that enterovirus replication complexes and viral particle lattices are present on or near to insulin granules in CVB acutely infected beta cells. Thus, this weight of evidence is strongly supportive of our hypothesis and deserves further study.

In summary, we show that human beta cells express the SIV isoform of CAR in the insulin granules. We propose that the biochemical properties of CAR-SIV that confer the physiological importance of this protein within beta cells may also represent an 'Achilles heel' by which the entry and replication of enteroviruses is facilitated.

Acknowledgements This research was performed with the support of the Network for Pancreatic Organ donors with Diabetes (nPOD; RRID:SCR_014641), a collaborative type 1 diabetes research project sponsored by the JDRF (nPOD: 5-SRA-2018-557-Q-R) and The Leona M. & Harry B. Helmsley Charitable Trust (Grant no. 2018PG-T1D053). Organ Procurement Organizations (OPO) partnering with nPOD to provide research resources are listed at http://www.jdrfnpod.org//for-partners/npod-partners/. The Biocenter Oulu electron microscopy core facility and T. Kantoluoto are acknowledged for cutting thin, frozen sections and assisting with staining. We would also like to acknowledge J. L. E. Hill (Institute of Biomedical & Clinical Science, University of Exeter Medical School, Exeter, UK) for assistance with the immunoprecipitations and J.-V. Turatsinze (ULB Center for Diabetes Research, Brussels) for bioinformatics support. Some of the data in this manuscript were presented at the Diabetes UK Professional Conference in 2017 (P14).

Data availability The datasets generated during and/or analysed during the current study are available from the corresponding author on reasonable request

Funding We are pleased to acknowledge financial support from the European Union's Seventh Framework Programme PEVNET (FP7/2007-2013) under grant agreement number 261441. The participants of the PEVNET consortium are described at http://www.uta.fi/med/pevnet/publications.html. Additional support was from a JDRF Career Development Award (5-CDA-2014-221-A-N) to SJR, a JDRF research grant awarded to the network of Pancreatic Organ Donors—Virus (nPOD-V) consortium (JDRF 25-2012-516), an MRC Project Grant MR/P010695/1 awarded to SJR, a Foundation main grant to EI from the

Funds for Women Graduates (178123), and FRFS-Welbio grant CR-2015A-06, Belgium, awarded to DLE.

Duality of interest The authors declare that there is no duality of interest associated with this manuscript.

Contribution statement SJR and NGM designed the study, performed data analysis and interpretation, and wrote the manuscript. EI MAR, SD, PL, GS, LN, DLE and VM performed data collection and analysis, and edited the manuscript. FD provided critical analysis of the results and edited the manuscript. All authors approved the manuscript's final version. SJR and NGM are the guarantors of this work and, as such, had full access to all the data in the study and take responsibility for the integrity of the data and the accuracy of the data analysis.

Figure Legends

Fig. 1 A description of the CAR isoforms and the selective expression of CAR-SIV in human islets. (**a**) CAR protein structure. The signal peptide (red) is cleaved to yield a mature protein with an ECD comprising two immunoglobulin (Ig)-like domains, type 1 (blue) and type 2 (green). The transmembrane domain (yellow) bridges the extracellular and cytoplasmic regions (pink), which terminates with a PDZ-binding domain (red). (**b**) *CXADR* exon maps of the five differentially spliced isoforms. The type 1 Ig domain is encoded by exons 2 and 3, while type 2 Ig-like domain is encoded by exons 4 and 5. Isoforms 1 and 2 contain a transmembrane domain and are named CAR-SIV (or hCAR1, CAR^{Ex7}) and CAR-TVV (or hCAR2, CAR^{Ex8}), respectively (denoted by the three terminal amino acids on their C-termini). The soluble isoforms 3, 4 and 5 are named CAR4/7, CAR3/7 and CAR2/7, respectively, reflecting exon inclusion or exclusion and lack of the transmembrane domain. The binding regions of the different CAR antibodies are also shown. The CAR-CT antiserum recognises amino acids 335–365 located at the C-terminus of the CAR-SIV isoform but does not recognise the other CAR isoforms. Both the CAR-ECD and CAR-RmcB antisera recognise epitopes within the ECD, and are predicted to recognise the majority of the longer CAR isoforms (CAR-SIV, CAR-TVV, CAR4/7 and potentially CAR3/7). (**c**, **d**) Representative immunocytochemical analysis of the expression of different CAR isoforms in normal control pancreas tissue stained with (**c**) CAR-CT and (**d**) CAR-ECD antisera. Scale bars, 20 μm. The insets below represent higher magnification images (of the areas outlined by the black boxes) demonstrating the differential staining profile of the CAR-CT antisera in the endocrine (+++) and exocrine pancreas (−), and the CAR-ECD antisera in the endocrine (+++) and exocrine pancreas (+); +++, strong; +, weak; –, negative. These results are representative of findings in pancreas from eight non-diabetic individuals; aa, amino acids, Ab., antibody

Fig. 2 Confirmation of SIV isoform expression in human islets. qRT-PCR analysis of *CXADR* isoform expression in (**a**) isolated human islets (*n*=5 individuals) and (**b**) LCM human islets (*n*=2 individuals) demonstrates that the SIV and TVV isoforms are highly expressed, CAR4/7 is present at low levels, and CAR3/7 and CAR2/7 are barely detectable. Data were normalised to the relative expression of three housekeeping genes β-actin, *GAPDH* and *B2M*. Relative expression is presented as the mean ± SEM. (**c**) RNAseq data showing CAR isoform expression in islets from five normoglycaemic individuals (mean ± SEM) [23]. RPKM, reads per kilobase of exon model per million mapped reads. (**d**) Confirmation of CAR-SIV protein expression in isolated human islets and EndoC-βH1 cells as assessed by western blotting using CAR-CT and CAR-ECD antisera and loading control GAPDH. H., human

Fig. 3 The SIV isoform of CAR is expressed in pancreatic beta cells. (**a**) Representative immunofluorescence staining of the CAR-SIV isoform (CAR-CT antibody; green), insulin (light blue), glucagon (red) and DAPI (dark blue) in an islet from a non-diabetic human pancreas. Scale bars, 10 μm. (**b**) CAR-SIV isoform staining in formalin-fixed, paraffin-embedded isolated human islets: CAR-SIV (CAR-CT; green) and insulin (red) and DAPI (dark blue). The enlarged region (from the area outlined by the dashed white box) demonstrates co-localisation of CAR-CT and insulin staining (yellow). Scale bars, 10 μm. (**c**) Granular distribution of CAR-SIV (green) and co-localisation with insulin (red) and DAPI (dark blue) in the islet of a non-diabetic pancreas. Scale bars, 5 μm. These results are representative of findings in the pancreases of 15 non-diabetic individuals (ESM Table 1)

Fig. 4 CAR-SIV co-localisation with multiple insulin granule proteins within the beta cell. Representative immunofluorescence staining of the CAR-SIV isoform (CAR-CT antibody; green) and insulin (blue) in relation to insulin secretory granule proteins (red) (**a**) ZnT8, (**b**) PC1/3 and (**c**) proinsulin. (**d**) Pearson correlation coefficient demonstrating the association between CAR-SIV and glucagon, insulin, ZnT8, PC1/3 and proinsulin, and between ZnT8 and

insulin. Each data point represents a single islet, and two islets were assessed per case from each of three independent samples. Representative higher magnification images of the CAR-SIV isoform (CAR-CT antibody; green) with (**e**) glucagon, (**f**) ZnT8, (**g**) PC1/3 and (**h**) proinsulin in red. DAPI is shown in dark blue. No association was observed between the CAR-SIV isoform (CAR-CT antibody; green) and glucagon (red) (**e**). Scale, bars 10 μm

Fig. 5 Cryoimmune electron microscopy. Immunogold labelling of CAR-SIV (10 nm gold particles) and ZnT8 (5 nm gold particles) in thin frozen sections of human pancreas tissue. (**a**) The low-magnification image demonstrates the presence of granules in acinar cells and in islet cells. (**b**, **c**) The higher magnification images (of the areas outlined by the dashed black boxes in **a**) reveal a lack of CAR-SIV labelling of acinar cell granules (**b**), but positive CAR-SIV labelling in beta cell granules (**c**). (**d**) A higher resolution, magnified image confirms that the labelling of CAR-SIV (10 nm gold; black arrows) and ZnT8 (5 nm gold; black arrowheads) surrounds the beta cell granules. Scale bars, 2 μm (**a**), 1 μm (**b**, **c**), and 500 nm (**d**). (**e**) Relative distribution of CAR-SIV in organelles based on quantification using line intersection counting. ER, endoplasmic reticulum

Fig. 6 CAR-SIV co-localisation with PICK1 in the beta cell. (**a**) Representative immunofluorescence staining of PICK1 (red), CAR-SIV isoform (CAR-CT antibody; green), insulin (light blue) and DAPI (dark blue) in non-diabetic human pancreas. Overlay of CAR-SIV and PICK1 (yellow), and CAR-SIV, PICK1 and insulin (white). (**b**) Pearson correlation coefficient demonstrating the extent of co-localisation of CAR-SIV with PICK1, CAR-SIV with insulin, and PICK1 with insulin. (**c**) Hyvolution imaging demonstrates a close association of the CAR-SIV isoform (CAR-CT antibody; green) and PICK1 (red) in the insulin granule (light blue) of a non-diabetic pancreas. Granules positive for insulin, PICK1 and CAR-SIV are indicated by the orange arrows. Scale bar, 5 μm

Fig. 7 CAR-SIV in beta cells. Our data demonstrate that CAR-SIV is present at high concentrations on the insulin granule and is closely associated with the cytoplasmic protein PICK1. CAR-SIV has previously been shown to interact with PICK1, which is proposed to have a role in the budding and maturation of vesicles from the *trans*-Golgi network. We predict that the C-terminus of CAR-SIV faces the extragranular/cytoplasmic environment since its PDZ-binding domain would be available to interact with cytoplasmic PICK1 only in this orientation. We propose that CAR-SIV, through its interaction with PICK1, could therefore play a hitherto unsuspected role in the maturation and trafficking of the insulin granule. Importantly, when considering the orientation of CAR-SIV in this model, the putative ECD of CAR-SIV, which is required for the binding of enteroviruses, faces the interior of the secretory granule during its maturation. This suggests that, as the insulin granule fuses with the plasma membrane during insulin exocytosis, the ECD of CAR-SIV becomes displayed on the external face of the plasma membrane and is then able to bind to enteroviruses that use this receptor, for example CVBs. During the subsequent endocytosis of the granule, for recycling, the virus would be transported inside the cell, where it could initiate a productive infection

References

[1] Yeung W-CG, Rawlinson WD, Craig ME (2011) Enterovirus infection and type 1 diabetes mellitus: systematic review and meta-analysis of observational molecular studies. Bmj 342: d35

[2] Frisk G, Diderholm H (2000) Tissue culture of isolated human pancreatic islets infected with different strains of coxsackievirus B4: assessment of virus replication and effects on islet morphology and insulin release. International journal of experimental diabetes research 1: 165-175

[3] Ylipaasto P, Klingel K, Lindberg AM et al. (2004) Enterovirus infection in human pancreatic islet cells, islet tropism in vivo and receptor involvement in cultured islet beta cells. Diabetologia 47: 225-239

[4] Roivainen M, Rasilainen S, Ylipaasto P et al. (2000) Mechanisms of coxsackievirus-induced damage to human pancreatic beta-cells 1. The Journal of Clinical Endocrinology & Metabolism 85: 432-440

[5] Richardson SJ, Willcox A, Bone A, Foulis AK, Morgan NG (2009) The prevalence of enteroviral capsid protein vp1 immunostaining in pancreatic islets in human type 1 diabetes. Diabetologia 52: 1143-1151

[6] Krogvold L, Edwin B, Buanes T et al. (2015) Detection of a low-grade enteroviral infection in the islets of Langerhans of living patients newly diagnosed with type 1 diabetes. Diabetes 64: 1682-1687

[7] Ylipaasto P, Smura T, Gopalacharyulu P et al. (2012) Enterovirus-induced gene expression profile is critical for human pancreatic islet destruction. Diabetologia 55: 3273-3283

[8] Richardson SJ, Leete P, Bone AJ, Foulis AK, Morgan NG (2013) Expression of the enteroviral capsid protein VP1 in the islet cells of patients with type 1 diabetes is associated with induction of protein kinase R and downregulation of Mcl-1. Diabetologia 56: 185-193

[9] Raschperger E, Thyberg J, Pettersson S, Philipson L, Fuxe J, Pettersson RF (2006) The coxsackie- and adenovirus receptor (CAR) is an in vivo marker for epithelial tight junctions, with a potential role in regulating permeability and tissue homeostasis. Experimental cell research 312: 1566-1580

[10] Bergelson JM, Cunningham JA, Droguett G et al. (1997) Isolation of a common receptor for Coxsackie B viruses and adenoviruses 2 and 5. Science (New York, NY) 275: 1320-1323

[11] Dörner A, Xiong D, Couch K, Yajima T, Knowlton KU (2004) Alternatively spliced soluble coxsackie-adenovirus receptors inhibit coxsackievirus infection. Journal of Biological Chemistry 279: 18497-18503

[12] He Y, Chipman PR, Howitt J et al. (2001) Interaction of coxsackievirus B3 with the full length coxsackievirus-adenovirus receptor. Nature structural biology 8: 874-878

[13] Excoffon KJ, Gansemer ND, Mobily ME, Karp PH, Parekh KR, Zabner J (2010) Isoform-specific regulation and localization of the coxsackie and adenovirus receptor in human airway epithelia. PloS one 5: e9909

[14] Cohen CJ, Shieh JT, Pickles RJ, Okegawa T, Hsieh JT, Bergelson JM (2001) The coxsackievirus and adenovirus receptor is a transmembrane component of the tight junction. Proc Natl Acad Sci U S A 98: 15191-15196

[15] Excoffon KJA, Hruska-Hageman A, Klotz M, Traver GL, Zabner J (2004) A role for the PDZ-binding domain of the coxsackie B virus and adenovirus receptor (CAR) in cell adhesion and growth. Journal of cell science 117: 4401-4409

[16] Kolawole AO, Sharma P, Yan R et al. (2012) The PDZ1 and PDZ3 domains of MAGI-1 Regulate the eight-exon isoform of the coxsackievirus and adenovirus receptor. Journal of Virology 86: 9244-9254

[17] Holst B, Madsen KL, Jansen AM et al. (2013) PICK1 deficiency impairs secretory vesicle biogenesis and leads to growth retardation and decreased glucose tolerance. PLoS Biol 11: e1001542

[18] Cao M, Mao Z, Kam C et al. (2013) PICK1 and ICA69 control insulin granule trafficking and their deficiencies lead to impaired glucose tolerance. PLoS Biol 11: e1001541

[19] Drescher KM, Kono K, Bopegamage S, Carson SD, Tracy S (2004) Coxsackievirus B3 infection and type 1 diabetes development in NOD mice: insulitis determines susceptibility of pancreatic islets to virus infection. Virology 329: 381-394
[20] Hodik M, Anagandula M, Fuxe J et al. (2016) Coxsackie–adenovirus receptor expression is enhanced in pancreas from patients with type 1 diabetes. BMJ Open Diabetes Research & Care 4: e000219
[21] Willcox A, Richardson SJ, Bone AJ, Foulis AK, Morgan NG (2009) Analysis of islet inflammation in human type 1 diabetes. Clinical & Experimental Immunology 155: 173-181
[22] Richardson SJ, Rodriguez-Calvo T, Gerling IC et al. (2016) Islet cell hyperexpression of HLA class I antigens: a defining feature in type 1 diabetes. Diabetologia 59: 2448-2458
[23] Eizirik DL, Sammeth M, Bouckenooghe T et al. (2012) The human pancreatic islet transcriptome: expression of candidate genes for type 1 diabetes and the impact of pro-inflammatory cytokines. PLOS Genetics 8: e1002552
[24] Slot JW, Geuze HJ (2007) Cryosectioning and immunolabeling. Nat Protoc 2: 2480-2491
[25] Ravassard P, Hazhouz Y, Pechberty S et al. (2011) A genetically engineered human pancreatic β cell line exhibiting glucose-inducible insulin secretion. The Journal of clinical investigation 121: 3589-3597
[26] Coyne CB, Bergelson JM (2006) Virus-induced Abl and Fyn kinase signals permit coxsackievirus entry through epithelial tight junctions. Cell 124: 119-131
[27] Robinson R (2013) A pair of crescent-shaped proteins shape vesicles at the golgi. PLoS biology 11:e1001543
[28] Arvan P, Pietropaolo M, Ostrov D, Rhodes CJ (2012) Islet autoantigens: structure, function, localization, and regulation. Cold Spring Harbor perspectives in medicine 2. doi: 10.1101/cshperspect.a007658.
[29] Hodik M, Skog O, Lukinius A et al. (2016) Enterovirus infection of human islets of Langerhans affects β-cell function resulting in disintegrated islets, decreased glucose stimulated insulin secretion and loss of Golgi structure. BMJ Open Diabetes Research Care 4: e000179

Fig. 1

a.

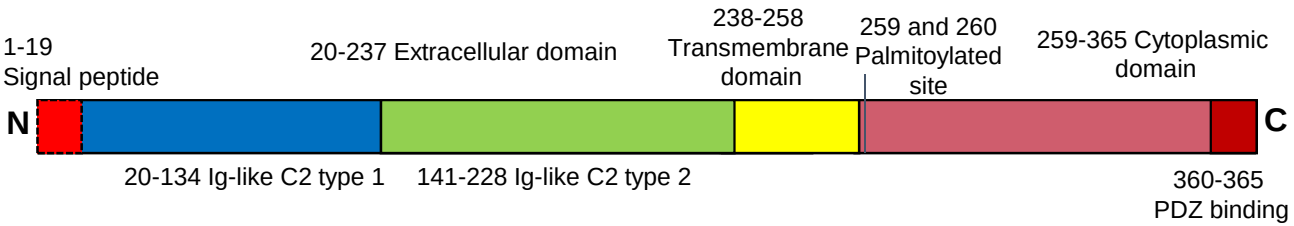

b

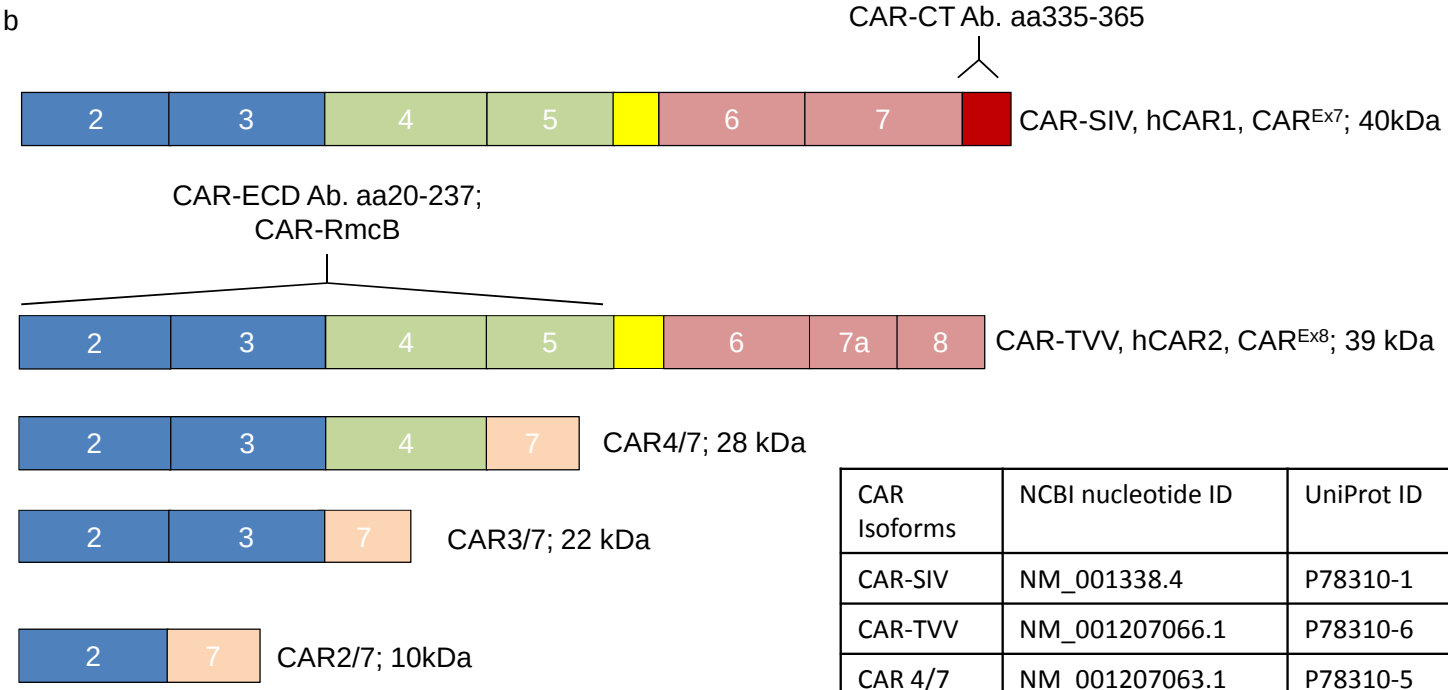

c.

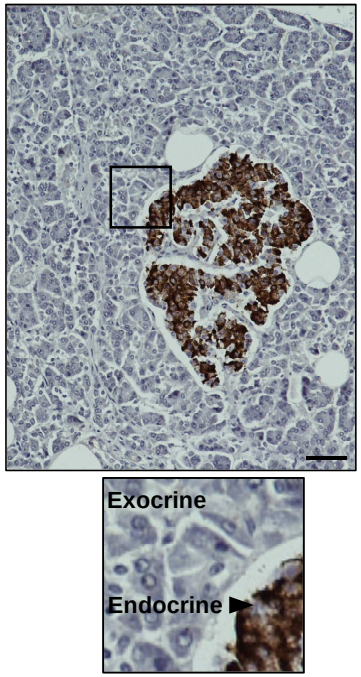

d.

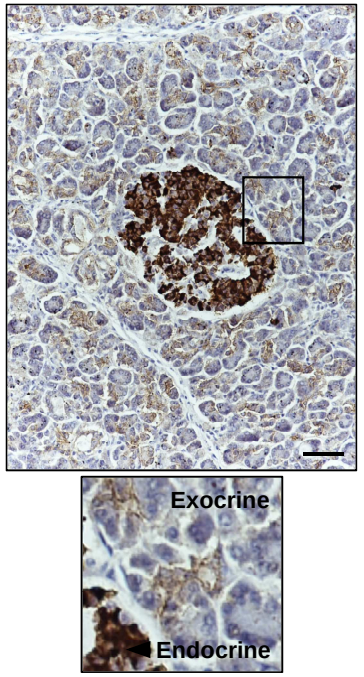

CAR Isoforms	NCBI nucleotide ID	UniProt ID
CAR-SIV	NM_001338.4	P78310-1
CAR-TVV	NM_001207066.1	P78310-6
CAR 4/7	NM_001207063.1	P78310-5
CAR 3/7	NM_001207064.1	P783104
CAR 2/7	NM_001207065.1	P783103

Fig. 2

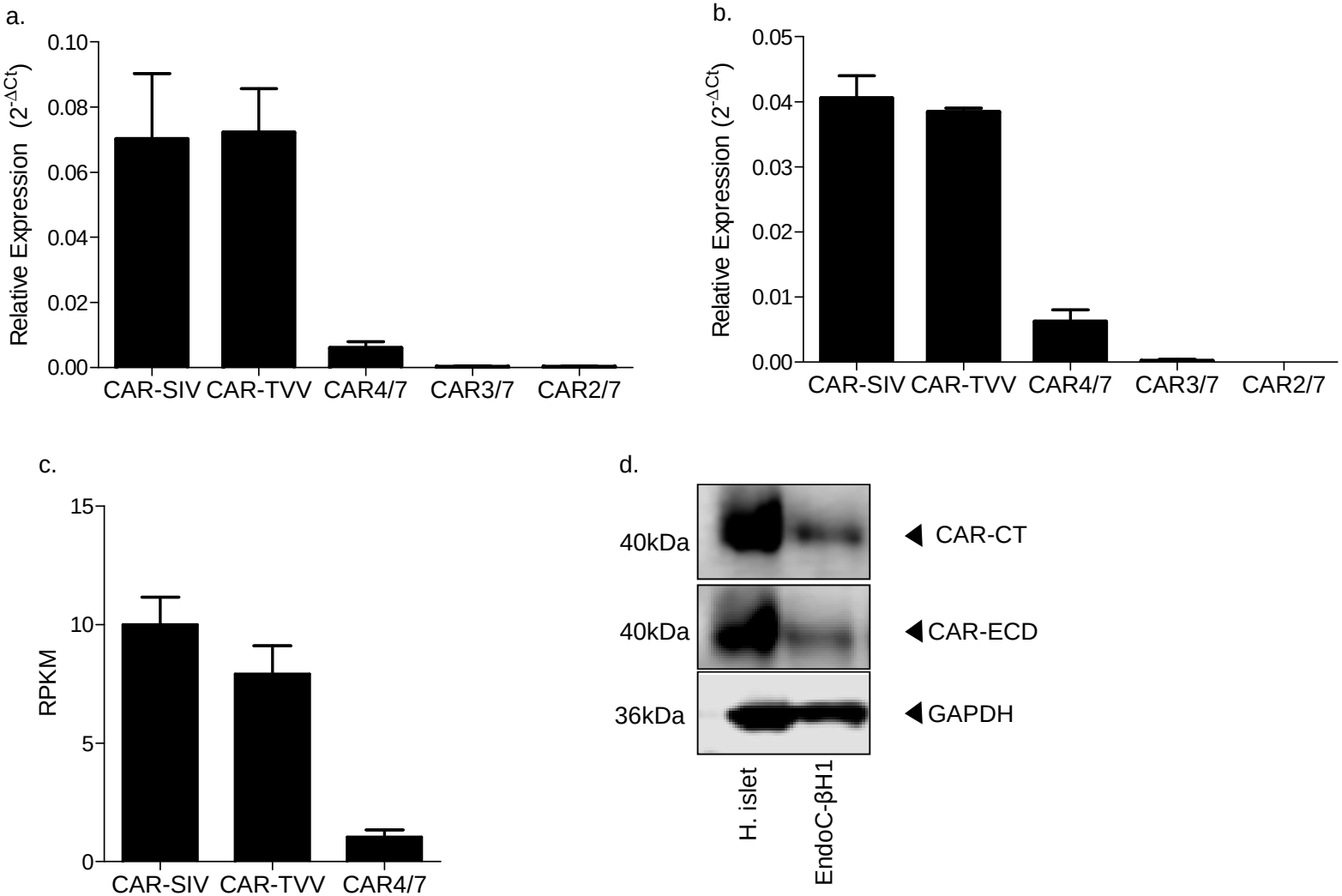
a.
Relative Expression ($2^{-\Delta Ct}$)
0.10
0.08
0.06
0.04
0.02
0.00
CAR-SIV
CAR-TVV
CAR4/7
CAR3/7
CAR2/7
b.
Relative Expression ($2^{-\Delta Ct}$)
0.05
0.04
0.03
0.02
0.01
0.00
CAR-SIV
CAR-TVV
CAR4/7
CAR3/7
CAR2/7
c.
RPKM
15
10
5
0
CAR-SIV
CAR-TVV
CAR4/7
d.
40kDa
CAR-CT
40kDa
CAR-ECD
36kDa
GAPDH
H. islet
EndoC-βH1

Fig. 3

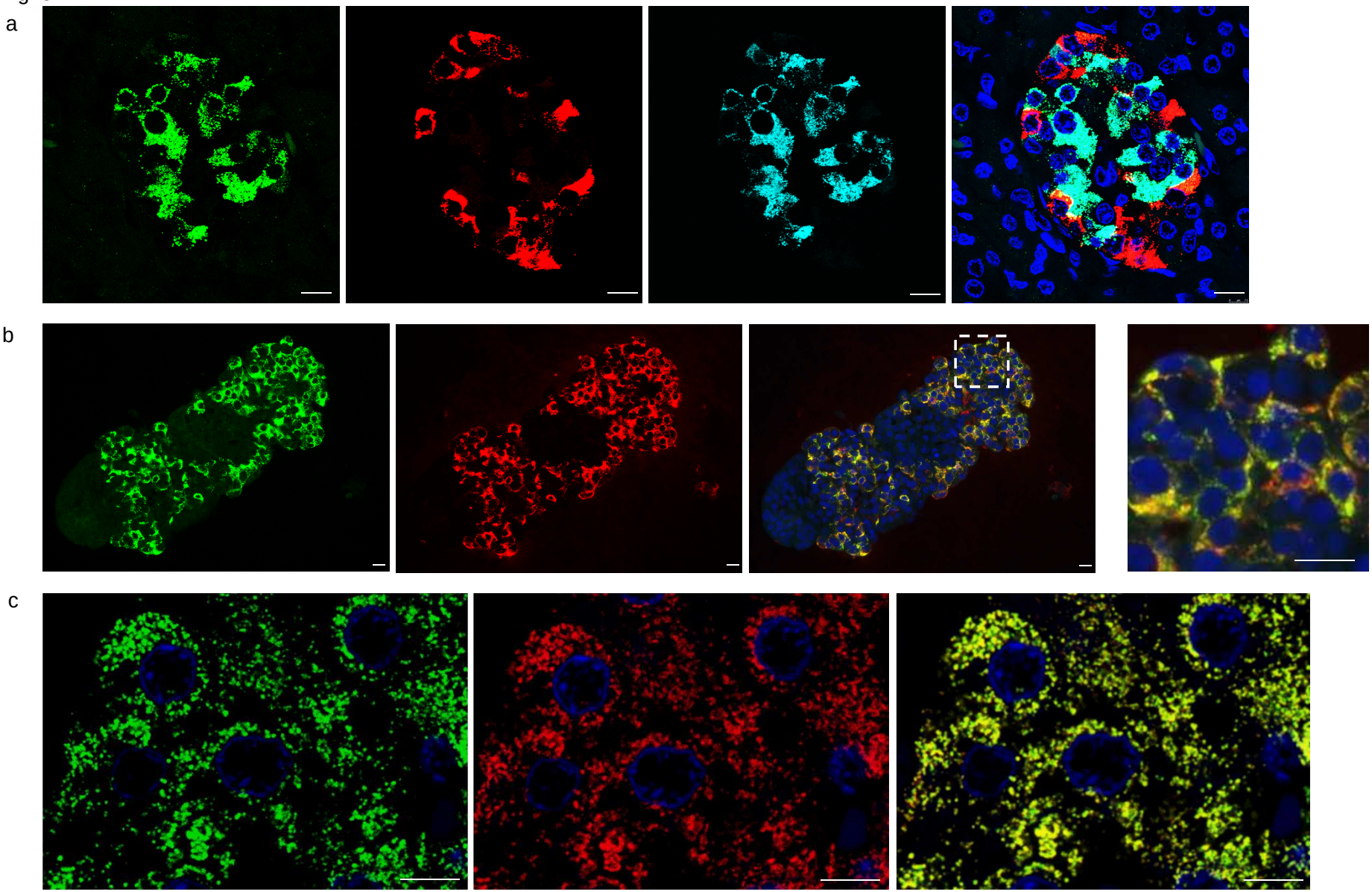

Fig. 4

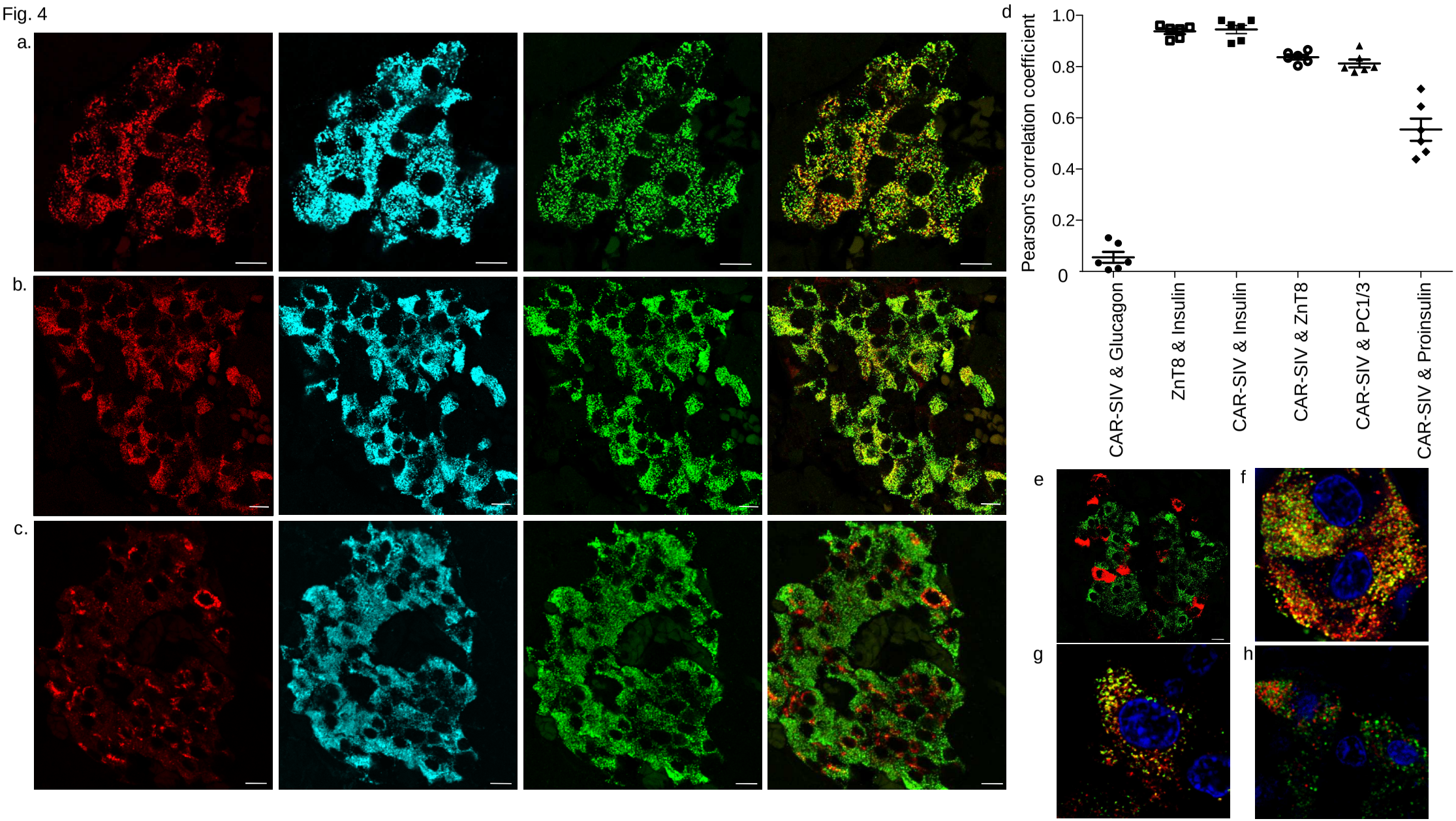
a.
b.
c.
d
Pearson's correlation coefficient
1.0
0.8
0.6
0.4
0.2
0
CAR-SIV & Glucagon
ZnT8 & Insulin
CAR-SIV & Insulin
CAR-SIV & ZnT8
CAR-SIV & PC1/3
CAR-SIV & Proinsulin
e
f
g
h

Fig 5

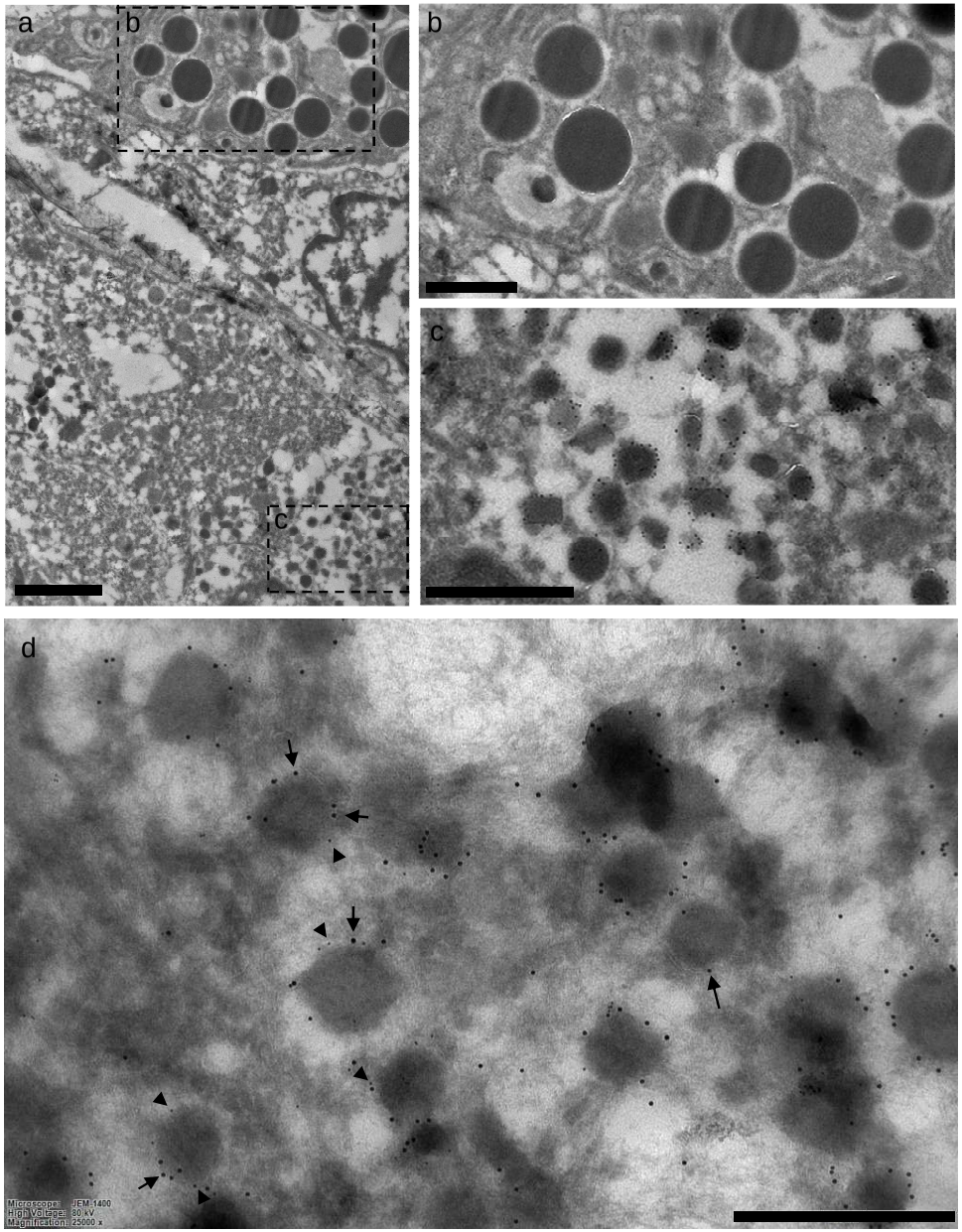
a
b
b
c
c
d
Microscope: JEM-1400
High Voltage: 80 kV
Magnification: 25000 x

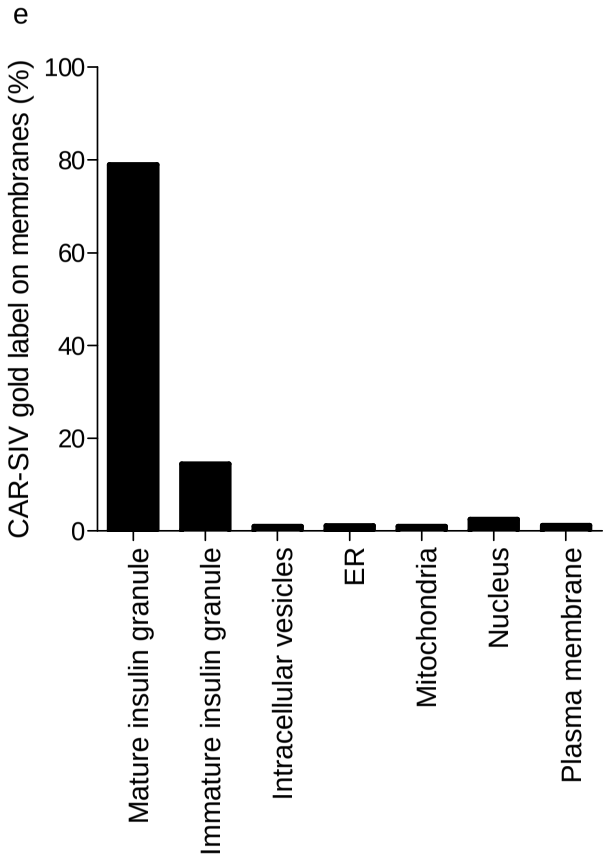
e
CAR-SIV gold label on membranes (%)
100
80
60
40
20
0
Mature insulin granule
Immature insulin granule
Intracellular vesicles
ER
Mitochondria
Nucleus
Plasma membrane

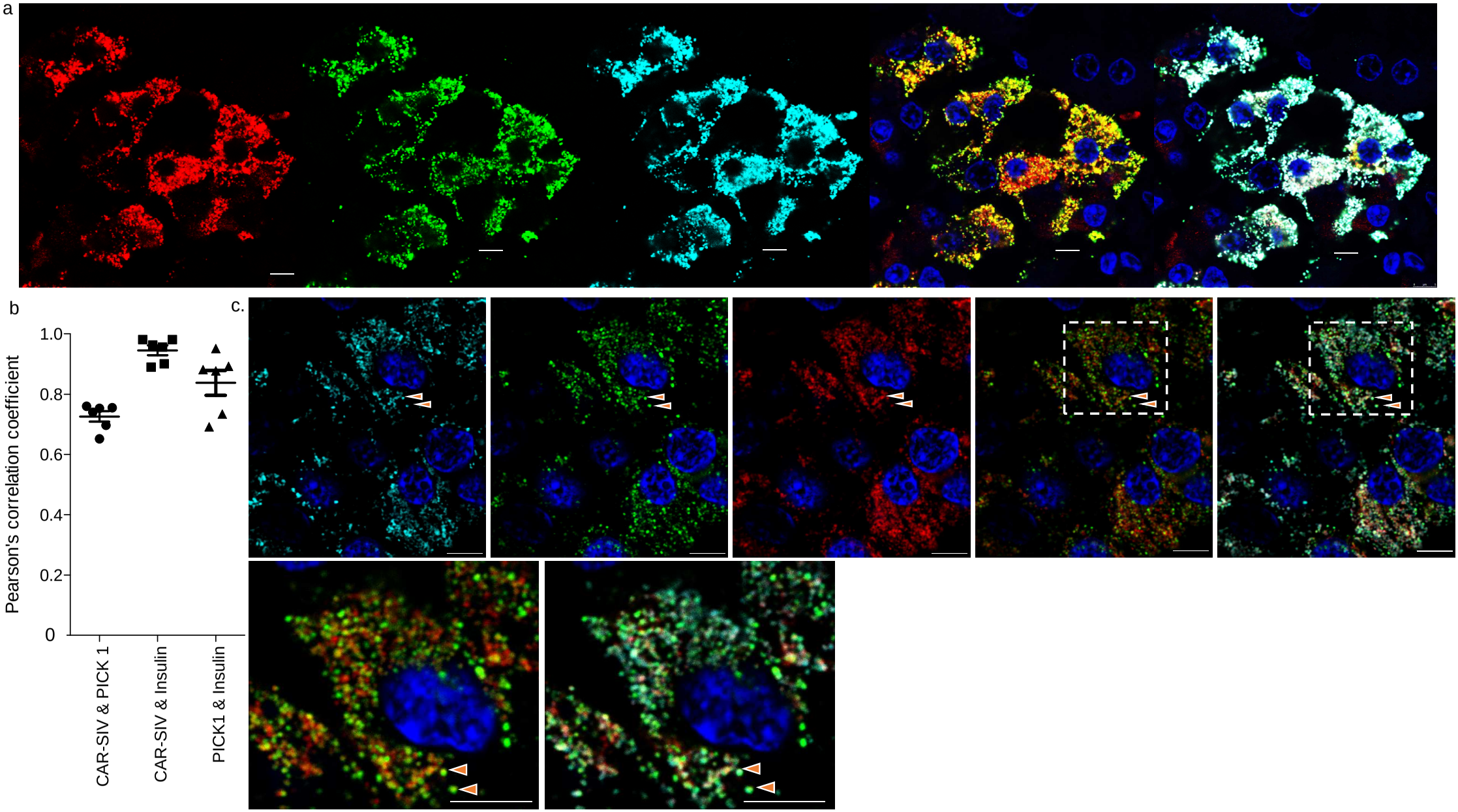
a
b
Pearson's correlation coefficient
1.0
0.8
0.6
0.4
0.2
0
CAR-SIV & PICK 1
CAR-SIV & Insulin
PICK1 & Insulin
c.

Fig. 7

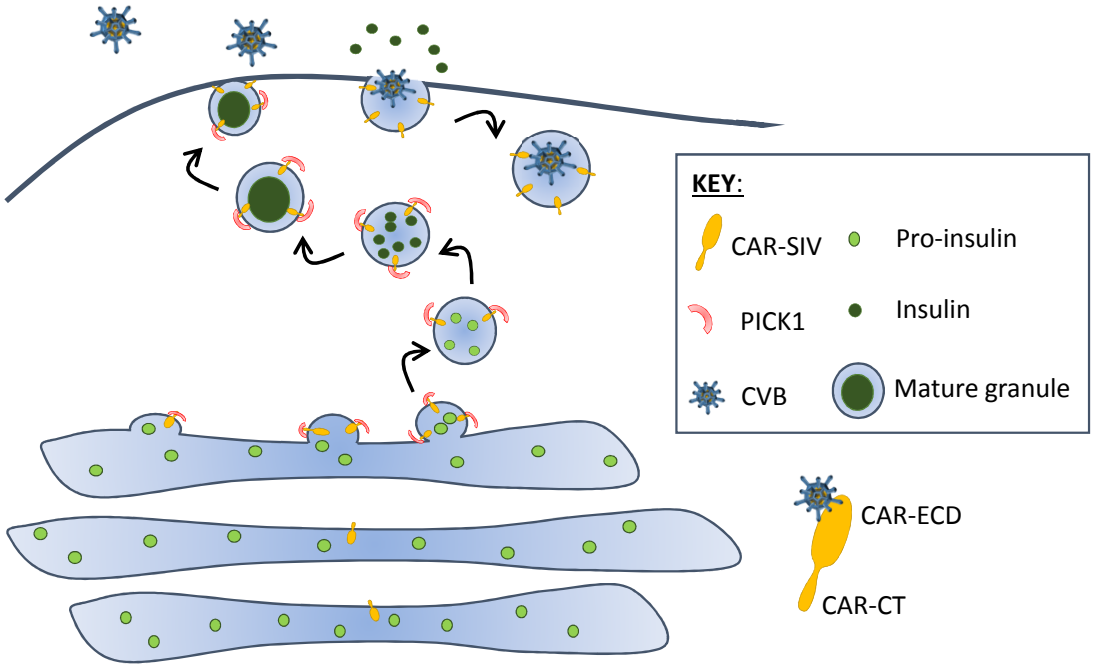
KEY:
CAR-SIV
Pro-insulin
PICK1
Insulin
CVB
Mature granule
CAR-ECD
CAR-CT

ESM METHODS:

Cell culture

The human beta cell line EndoC-βH1 (kindly provided by Dr. R. Scharfmann, University of Paris, France (1) was cultured in Matrigel-fibronectin-coated plates as described (2). Cells were cultured in DMEM containing 5.5mmol/l glucose, 2% bovine serum albumin (fraction V), 50μmol/l β-mercaptoethanol, 5.5μg/ml transferrin, 6.7ng/ml sodium selenite, 10mM nicotinamide, penicillin (100units/ml) and streptomycin (100μg/ml). Cells were seeded at 1.75 $x10^6$/ml on an extracellular matrix (ECM) with fibronectin coated T25 flasks and were sub-cultured every 7-9 days. Half of the culture medium was replaced every 3-4 days. Human 1.1B4 cells which were a gift from Prof. Peter Flatt (3) were cultured in RPMI 1640 medium containing 11.1mM glucose and supplemented with 10% fetal bovine serum, 2mmol/l L-Glutamine, 100U/ml penicillin and 100μg/ml streptomycin.1.1B4 cells were sub-cultured upon reaching 80% confluence and both cell lines were maintained at 37^0C, 100% humidity and 5% CO_2. All cells were mycoplasma negative.

Mutagenesis

A pCMV6 vector containing the SIV isoform of the human *CXADR* gene with a Myc-DDK tag was purchased (ORIGENE Rockville, MD, USA).The $Q5^R$ site directed mutagenesis kit was used according to the manufacturer's instruction (New England Biolabs, Hitchin, UK) to produce truncated variants of the protein encoded by the cDNA. Primers were synthesized to generate the SIV isoform without a Myc-DDK tag (F: GTCTATAGTATAGCGTACGCGGCC; R: CCATCCTTGCTCTGTGCT) or without the final three amino acids of the isoform (F: GACCAAGGATTAGTCTATAGTAACG; R:

TGTGCTGGAATCATCACAG). All variants were fully sequenced to confirm the success of mutagenesis (Source Bioscience, Nottingham, UK).

Western blotting

Cells were collected and lysed in buffer (20mmol/l Tris, 150mmol/l Nacl, 1mM EDTA and 1% Triton-X including protease and phosphatase inhibitors (Sigma, Poole, UK)) on ice for 10mins. Protein lysates was separated from insoluble fraction by centrifugation at 5000rpm for 10mins at 4^0C. Total protein was estimated with the Pierce ^{TM} (BCA) Protein Assay (Thermofisher Scientific, UK) and absorbance was measured at 562nm with a PHERAstar (BMG Labtech). Equal amount of proteins (20-50ug) were adjusted with 25% of 4x lithium dodecyl sulphate (LDS) loading buffer and 10% β-mercaptoethanol prior to denaturing at 70^{o}C for 10mins. Protein samples were loaded onto a pre-cast 12% Bis-Tris poly-acrylamide gel (Invitrogen) and electrophoresis was carried out using XCell Sure Lock (Invitrogen) at 120V in 20x MOPS SDS running buffer (Invitrogen) for 1hr. Proteins were electro-transferred onto a methanol permeabilized polyvinylidene difluoride (PVDF) membrane using XCell II Blot Module (Invitogen, UK) containing transfer buffer (Glycine, Tris, Methanol, ddH20) at 30V for 2hrs.

Membranes were blocked in 5% skimmed milk (Sigma) in Tris buffered saline with 0.05% Tween 20 (TBST) buffer at room temperature for 1hr. Primary antibodies; anti-CAR-CT (1:1000, ab100811, Abcam), anti-CAR-ECD (1:500, ab180761, Abcam), β-actin (1:10000, A5441, Sigma), anti-PICK1 (1:1000, Abcam ab133773) or GAPDH (1:10000, 60004-1-Ig, Proteintech) were diluted in 5% milk/ TBST and membranes probed overnight at 4^0C, with the exception of β-actin and GAPDH (2hrs at room temperature). The membrane was washed 3x with TBST and probed with a secondary antibody raised against mouse or rabbit conjugated to Alkaline phosphatase (A3562, A3687, Sigma) or Goat anti-rabbit IgG (H+L) highly crossed

absorbed, Alexafluor plus 680 (#A327-34, Thermofisher) in 1% milk/ TBST for 1hr at room temperature. Finally, the membrane was washed 3x with TBST and bands were visualised with a CDP-Star Chemiluminescent substrate (Sigma, C0712) using either a Li-COR C-Digit or Odyssey CLX (Li-COR Biosciences, UK)

Flow cytometry

Cells were trypsinised and re-suspended in FACS buffer (PBS, 2% FBS). For intracellular staining, cells were fixed with 4% paraformaldehyde, washed twice with FACS buffer and incubated with either anti-CAR CT or anti-CAR-RmCB-PE (FCMAB418PE, Merck Millipore) or negative control antibodies. Rabbit Isotype IgG (I-1000 Vector laboratories) or Mouse IgG1k (FCMAB230P, Merck) in 0.3% saponin at 4^0C for 45mins. Cells were then washed in 0.03% saponin in FACS buffer and then analysed immediately on a Flow cytometer (BD Accuri ^{TM} C6 Plus) or if they were not directly conjugated to a fluorochrome, they were incubated with secondary antibody (Alexa-488) for 30mins prior to analysis. For extracellular staining, cells were incubated with either CAR-CT or CAR-Rmcb-PE in FACS buffer at room temperature for 45mins. Cells were then washed in FACS buffer and analysed or incubated with secondary antibodies (Alexa-488) before analysis. Results were confirmed in 3 independent experiments.

Laser capture microdissection of human islets

Laser capture microdissection (LCM) of human islets was performed on OCT frozen sections from pancreas of non-diabetic nPOD donors (6017, 6096; Supplementary Table 4). Briefly, 5µm thick frozen sections were fixed in 70% ethanol for 30 seconds and then dehydrated in 100% ethanol, xylene and then air dried for 5 minutes. An Arcturus Xt microdissection

instrument (Thermofisher, Waltham, MA, USA) was used to capture human islets based on beta-cell autofluorescence. Hs-Caps (Thermofisher) were used to microdissect identified islets. Microdissected islets were then lysed in Arcturus Picopure kit Extraction Buffer for 30 minutes at 42°C and subjected to total RNA extraction using Arcturus Picopure RNA extraction kit following the manufacturer's instructions (Thermofisher).

Real Time RTqPCR

Total RNA from isolated human islets was extracted using miRNeasy mini kit (Qiagen, Hilden, Germany). Briefly, human isolated islets were lysed in Qiazol solution and chloroform was added to separate DNA, RNA and proteins. The aqueous phase was then loaded on to RNA binding columns and eluted in 30µl of nuclease-free water. RNA quality were evaluated using a 2100 Bioanalyzer RNA 6000 Pico kit (Agilent Technologies, Santa Clara, CA, USA) and only samples with RNA Integrity Number (RIN) >5.0 were used for further analyses.

Differential expression of alternatively spliced isoforms of the human *CXADR* gene were evaluated using custom designed TaqMan primers and probes (Thermofisher) (ESM Table 3). For human isolated islets (ESM Table 4), 250ng of total RNA was retro-transcribed using Superscript III Reverse Transcriptase kit (Thermofisher) and 10ng of the resultant cDNA were loaded into 2x TaqMan Universal Master Mix, 20x TaqMan gene expression assay buffer and nuclease-free water in a final volume of 20µl. Data were normalised using the expression of β-Actin, GAPDH and β2-microglobulin. Reactions were performed on a Verity Thermal Cycler and ViiA7 Real Time PCR instruments (Thermofisher). Data were analysed and exported using Expression Suite software 1.1 (Thermofisher) and finally elaborated using the $2^{-\Delta Ct}$ method.

For LCM captured islets (ESM Table 5), 1ng of total RNA was retro-transcribed using Superscript III Reverse Transcriptase kit (Thermofisher). The resultant cDNA was pre-amplified using 0.2x Tris-EDTA-diluted TaqMan assays pool (designed to amplify *CXADR* isoforms plus 3 housekeeping genes (β-Actin, GAPDH, β2-microglobulin)) and 2x Preamp Master Mix in a final volume of 50µl. The pre-amplification reaction was diluted in Tris-EDTA and 5µl of each pre-amplified cDNAs were used in a Real-Time PCR reaction in a final volume of 20µl.

Semi-quantitative RT-PCR

Total RNA was isolated from human islets (ESM Table 4) using RNeasy mini kits (Qiagen, Manchester, UK). 1µg of RNA was reverse transcribed (Promega, Madison,WI, USA) to synthesize cDNA. Specific primers were designed to selectively target the two *CXADR* transmembrane isoforms; CAR-SIV (F: GGAAGTTCATCACGATATCAG; R:AATCATCACAGGAATCGCAC), CAR-TVV (F: GGAAGTTCATCACGATATCAG; R: TTCCATCAGTCTTGTAAGGG). Amplified bands were excised and sequenced (Source Bioscience, Nottingham, UK) to confirm the isoform expression pattern.

Cryo-immune EM

For cryo-immuno-EM human samples were treated as described [24]. Briefly, human pancreas tissue samples (nPOD 6227, 6229 and 6330) were fixed in 4% PFA, cut into small pieces and immersed in 2.3 mol/l sucrose in PBS at 4°C. The samples were placed on metal stubs, frozen in liquid nitrogen and thin cryosections were cut and protected with sucrose/methyl cellulose films. For immunolabeling, the protective layer was first melted in gelatin coated dishes at 37°C and then washed with 0.1% glycine in PBS. Then grids were incubated in PBS containing 1% BSA with appropriate antibodies (ESM Table 2) for 45 minutes at room temperature.

Protein A-gold labelled antibodies (diameters 5, 10 or 20nm; G. Posthuma, Utrecth) diluted in 0.1% BSA in PBS was added onto the grids for 20 min followed by washes with 0.1% BSA/PBS and PBS alone. A bridging antibody was used to link the proinsulin to the 20nm gold particles. In double or triple labelling studies, antibodies were added sequentially with their respective protein-A gold conjugate, between incubations the sections were incubated briefly with 1% glutaraldehyde. The sections were then stained with 2% neutral uranyl acetate in water for 5 min and embedded for 10 min on ice with 2% methylcellulose containing 0.4% uranyl acetate and examined with a Jeol 1400 microscope.

Quantification of CAR-SIV in Cryo-immune EM

Quantification of CAR-CT immuno-gold labelling was performed by conventional line intersection counting from electron micrographs of human pancreas sections labelled with anti-CAR-CT (4). The same array of test lines was overlaid at random positions on all micrographs. Intersections with membrane limited compartments (mature and immature secretory granules, exocrine granules, endoplasmic reticulum, mitochondria, nucleus and plasma membrane) were assessed and the gold particles in these specific intersections counted. 21 micrographs were analysed yielding a total of 841 gold particles and 1291 intersections between membrane compartments. Numbers of gold particles per intersection were calculated and normalized for the abundance of each relevant compartment. Data were then displayed as the percentage of CAR-SIV gold particles in each of the different compartments. For ESM Fig 6, the number of CAR-SIV positive granules that were also labelled with proinsulin and/ or insulin labelled gold particles were counted.

Co-immunoprecipitation of PICK1 with CAR

Whole cell extracts were prepared by lysing 5 x 10^5 EndoC-βH1 cells or human islets with buffer containing 50mmol/l Tris (pH 7.5); 137mmol/l NaCl; 5mmol/l EDTA; 1mmol/l EGTA; 10µg/ml protease inhibitor (Sigma) and 10µg/ml phosphatase inhibitor cocktail 2 & 3 (Sigma, UK). The lysates were incubated with 3µg of anti-CAR clone RmcB or negative control mouse IgG (Dako; X0931) overnight at 4^0C. Protein G Sepharose beads were then added for 4 hours at 4^0C followed by three washes [first - lysis buffer; second -10% lysis buffer in TBS (50mmol/l Tris (pH 7.5) and 137mmol/l NaCl); Third – TBS). Proteins were eluted with 4x LDS and 10% β-mercaptoethanol at 70^0C for 10min. Western blot analysis was then performed as described above.

ESM Table 1: Tissue Samples, Patient Information

Case ID	Case Type	Cohort	Age	Sex	Duration of disease
12425	No diabetes	EADB	Neonate	N/A	
8582	No diabetes	EADB	1	N/A	
150/88	No diabetes	EADB	3	F	
274/91	No diabetes	EADB	6	M	
245/90	No diabetes	EADB	6	M	
8651	No diabetes	EADB	6	N/A	
12229	No diabetes	EADB	10	N/A	
540/91	No diabetes	EADB	11	M	
6099-06	No diabetes	nPOD	14.2	M	
PM146/66	No diabetes	EADB	18	F	
PAN 8	No diabetes	EADB	19	N/A	
PAN 1	No diabetes	EADB	22	N/A	
6160-06	No diabetes	nPOD	22.1	M	
329/72	No diabetes	EADB	24	M	
191/67	No diabetes	EADB	25	M	
PM132/67	No diabetes	EADB	46	M	
330/71	No diabetes	EADB	47	M	
186/74	No diabetes	EADB	55	F	
77/6/87	No diabetes	EADB	57	F	
332/66	No diabetes	EADB	59	M	
6098	No diabetes	nPOD	17.8	M	
6153	No diabetes	nPOD	15.2	M	
6027	AAb+	nPOD	18.8	M	
6167	AAb+	nPOD	37	M	
E236	T1D	EADB	7	F	'Recent'
SC41	T1D	EADB	4	F	3 weeks
11746	T1D	EADB	6	M	<1 week
11713	T1D	EADB	3	M	3mth
E375	T1D	EADB	11	F	1 week
E560	T1D	EADB	42	F	18mths
6041	T1D	nPOD	26.3	M	23y
6087	T1D	nPOD	17.5	M	4y
6113	T1D	nPOD	13.1	F	1.58y
6161	T1D	nPOD	19.2	F	7y

EADB – Exeter Archival Diabetes Biobank; AAb+ - Autoantibody positive no diabetes; N/A – not avaliable

ESM Table 2: Antibody Details and Conditions for IHC/ IF. All antisera were validated with positive and negative controls and the CAR antisera were further validated (ESM Fig 1)

Primary Antibody	Manufacturer and clone	IHC/IF Antigen Retrieval	Conditions and Secondary Detection System
CAR-CT	Abcam ab100811 Rabbit polyclonal	10mmol/l citrate pH6.0	Dako REAL Envision Detection System or Immunofluorescence staining (1/1000 for 1hr) using anti-rabbit IgG (H+L) Alexa Fluor-conjugated secondary antibodies (1/400 for 1hr)
CAR-ECD	Abcam ab180761 Rabbit polyclonal	10mmol/l citrate pH6.0	Dako REAL Envision Detection or Immunofluorescence staining (1/200 for 1hr) using anti-rabbit IgG (H+L) Alexa Fluor-conjugated secondary antibodies (1/400 for 1hr)
CAR RmcB	Merck #05-644 Lot # 2880699 Mouse monoclonal	Utilised for ICC and IP	ICC Immunofluorescence staining (1/400 for 1hr) using anti-mouse IgG (H+L) Alexa Fluor-conjugated secondary antibodies (1/400 for 1hr)
Insulin	Dako C#A0564 Guinea-pig polyclonal	10mmol/l citrate pH6.0	Immunofluorescence staining (1/700 for 1hr) using anti-guinea-pig IgG (H+L) Alexa Fluor-conjugated secondary antibodies (1/400 for 1hr)
Glucagon	Abcam C#ab82270 Mouse monoclonal	10mmol/l citrate pH6.0	Immunofluorescence staining (1/2000 for 1hr) using anti-mouse IgG (H+L) Alexa Fluor-conjugated secondary antibodies (1/400 for 1hr)

Proinsulin	Abcam ab8301 Mouse monoclonal	10mmol/l citrate pH6.0	Immunofluorescence staining (1/500 for 1hr) using anti-mouse IgG (H+L) Alexa Fluor-conjugated secondary antibodies (1/400 for 1hr)
ZnT8	R & D C#815039 Mouse monoclonal	10m mmol/l citrate pH6.0	Immunofluorescence staining (1/63 for 1 hr) using anti-mouse IgG (H+L) Alexa Fluor-conjugated secondary antibodies (1/400 for 1hr)
PC1/3	Abcam Ab55543 Mouse monoclonal	10m mmol/l citrate pH6.0	Immunofluorescence staining (1/500 for 1hr) using anti-mouse IgG (H+L) Alexa Fluor-conjugated secondary antibodies (1/400 for 1hr)
PICK1	Santa Cruz	10m mmol/l Citrate pH6.0	Immunofluorescence staining (1/50 for 1hr) using anti-mouse IgG (H+L) Alexa Fluor-conjugated secondary antibodies (1/400 for 1hr)

ESM Table 3: TaqMan Probe Sequences

Target sequence	Probe ID	Taqman Probe Sequence
CXADR EXON_2_7	AIKAMSZ	ggtggatcaagtgggaagat
CXADR EXON_3_7	AILJKY7	gtagttcttgggaagatgtg
CXADR EXON_4_7	AIMSI5F	catggttagcagggaagatg
CXADR EXON_6_7 (CAR-SIV)	AIN1HBN	cgatatcagggaagatgtgc
CXADR EXON_6_7_8 (CAR-TVV)	AIPAFHV	ccaacatggaaggatattcc

ESM Table 4: Human islet donors, samples used for TaqMan qRT-PCR

Sample ID	Gender	Age (y)	BMI (Kg/m^2)
1	M	52	34.2
2	M	50	27.4
3	M	55	28.0
4	F	79	23.9
5	M	59	26.7

ESM Table 5: Donor information for LCM islet isolation

Sample ID	Gender	Age (y)	BMI (Kg/m^2)	No. Of LCM captured islets	RIN Value
6017	F	59	24,8	52	5.1
6096	F	16	18,8	39	7.2

References

(1) Ravassard P, Hazhouz Y, Pechberty S, Bricout-Neveu E, Armanet M, Czernichow P, Scharfmann R: A genetically engineered human pancreatic β cell line exhibiting glucose-inducible insulin secretion. The Journal of clinical investigation 2011;121:3589-3597

(2) Brozzi F, Nardelli TR, Lopes M, Millard I, Barthson J, Igoillo-Esteve M, Grieco FA, Villate O, Oliveira JM, Casimir M, Bugliani M, Engin F, Hotamisligil GS, Marchetti P, Eizirik DL: Cytokines induce endoplasmic reticulum stress in human, rat and mouse beta cells via different mechanisms. Diabetologia 2015;58:2307-2316

(3) McCluskey JT, Hamid M, Guo-Parke H, McClenaghan NH, Gomis R, Flatt PR: Development and functional characterization of insulin-releasing human pancreatic beta cell lines produced by electrofusion. Journal of Biological Chemistry 2011;286:21982-21992

(4) Griffiths G (1993) Fine Structure Immunocytochemistry. Heidelberg, Springer. DOI 10.1007/978-3-642-77095-1.

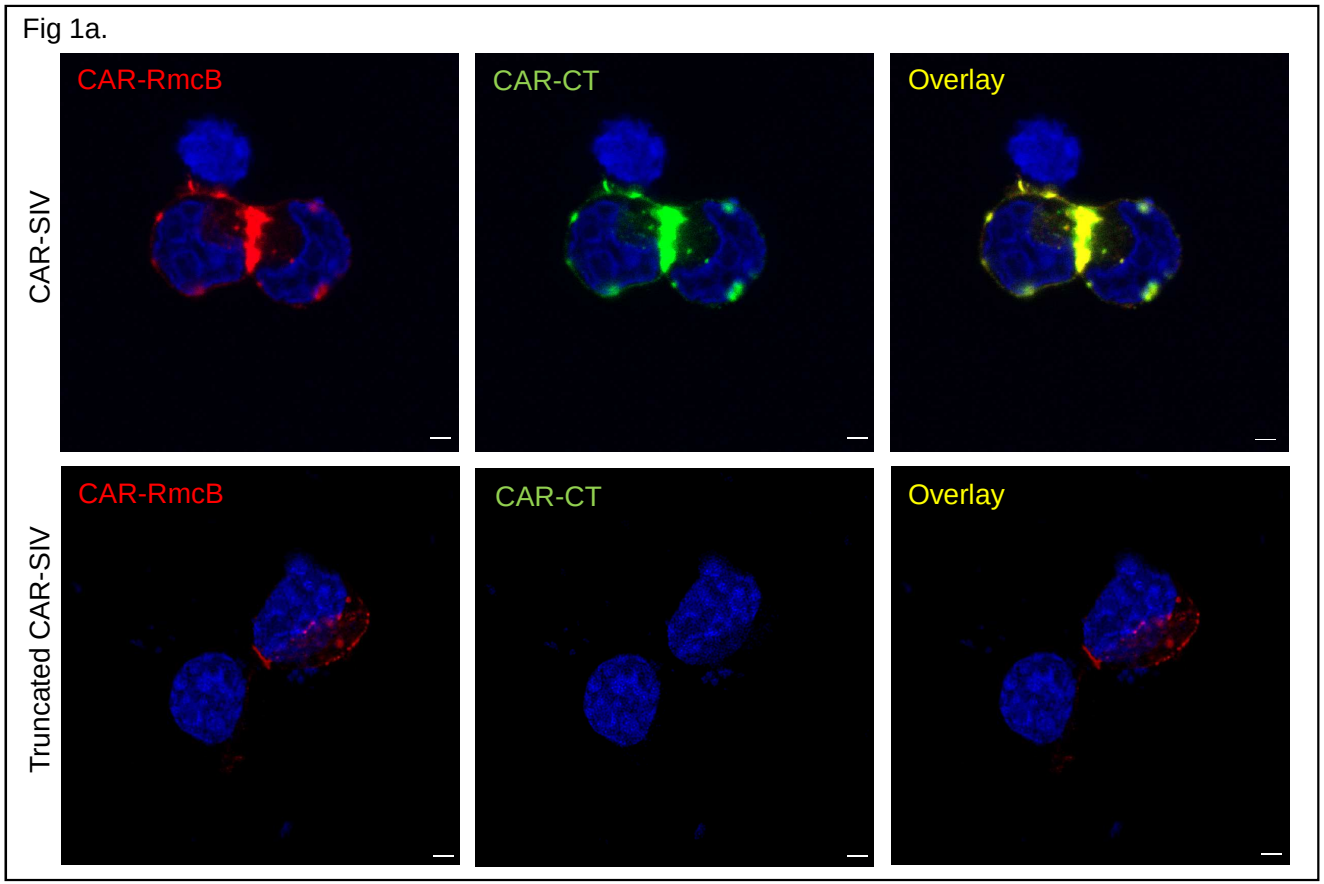

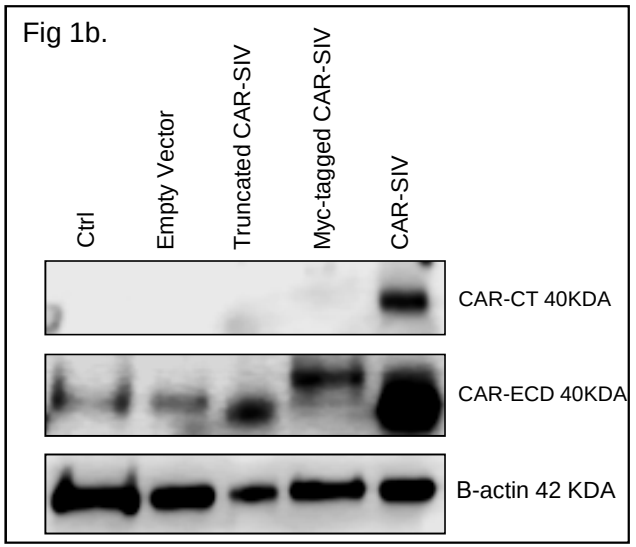

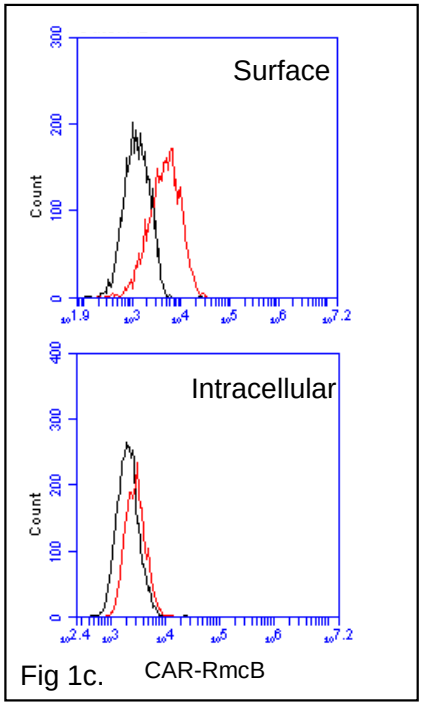

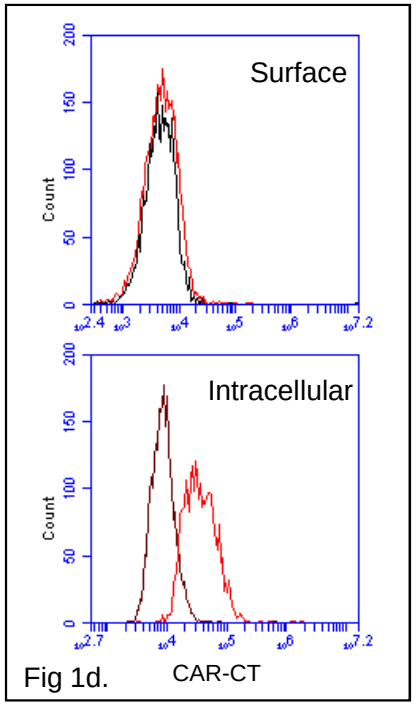

ESM Fig. 1: Analysis of CAR antibody specificity. (a) 1.1B4 cells (see Supplementary methods) were transfected with either the full length CAR-SIV (upper panel) or truncated CAR-SIV (lower panel) and probed with CAR-RmcB (red) or CAR-CT (green) antisera. Scale bar 2.5μm. The full length CAR-SIV is recognised by both the CAR-CT and the CAR-RmcB antisera. In contrast, the truncated CAR-SIV is only recognised by the CAR-RmcB antiserum, demonstrating the absolute requirement for the terminal three amino acids for CAR-CT antiserum binding. **(b)** Western blot analysis confirms that CAR-CT antisera detects only the full length CAR-SIV (40kDa) isoform in transfected 1.1B4 cells. Cells transfected with either the truncated CAR-SIV or the Myc-tagged CAR-SIV (where the Myc-tag immediately at the C teminus appears to hinder antibody access) are not recognised by the CAR-CT antiserum. In contrast the CAR-ECD antibody that detects the ECD of CAR can recognise other CAR isoforms including CAR-TVV (40kDa) visible in control and empty vector cells, as well as the CAR-SIV shown in the truncated CAR-SIV, Myc-tagged CAR-SIV and the full length CAR-SIV transfected cells. Representative flow cytometry plots of **(c)** CAR-RmcB and **(d)** CAR-CT antisera staining of the surface (upper panels) and intracellular expression (lower panels) on EndoC-βH1 cells.

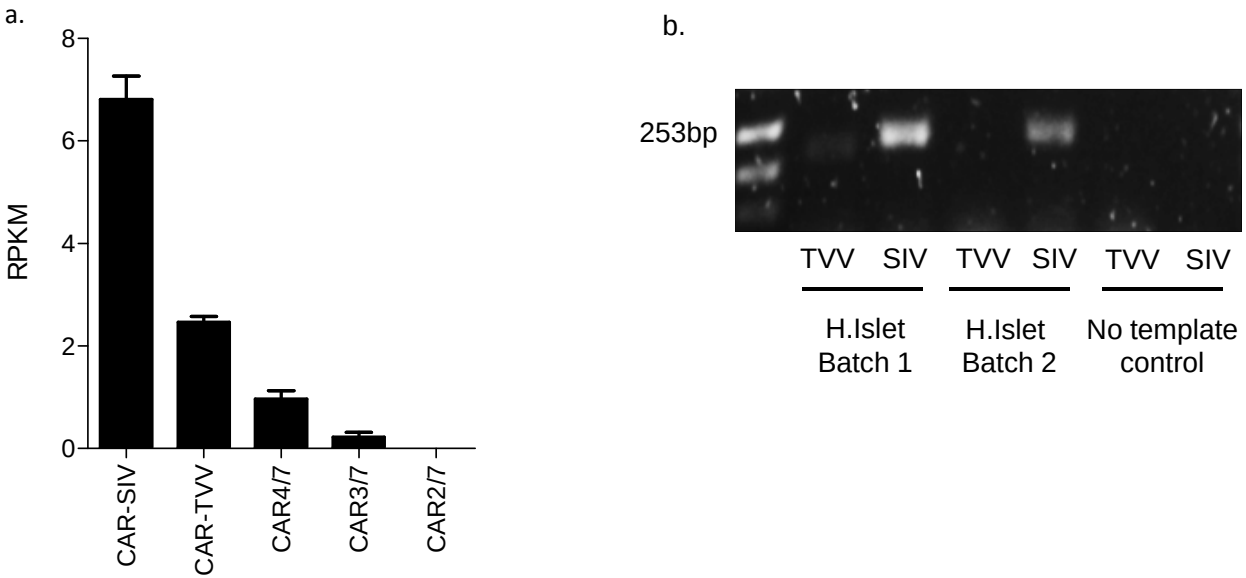

ESM Fig. 2: (a) RNAseq analysis of CAR isoform expression in 5 preparations of the human pancreatic beta cell line (ESM Table 4), EndoC-βH1 (Mean±SEM). CAR-SIV is expressed at levels 3-fold higher than CAR-TVV. CAR4/7 and CAR3/7 are present at low levels and CAR2/7 was undetectable. **(b)** Semi-quantitative RT-PCR (30 cycles) analysis using specific CAR-SIV and CAR-TVV primers in RNA extracted from purified human islets, suggests in two independent islet preparations that CAR-SIV is present at a higher abundance than CAR-TVV.

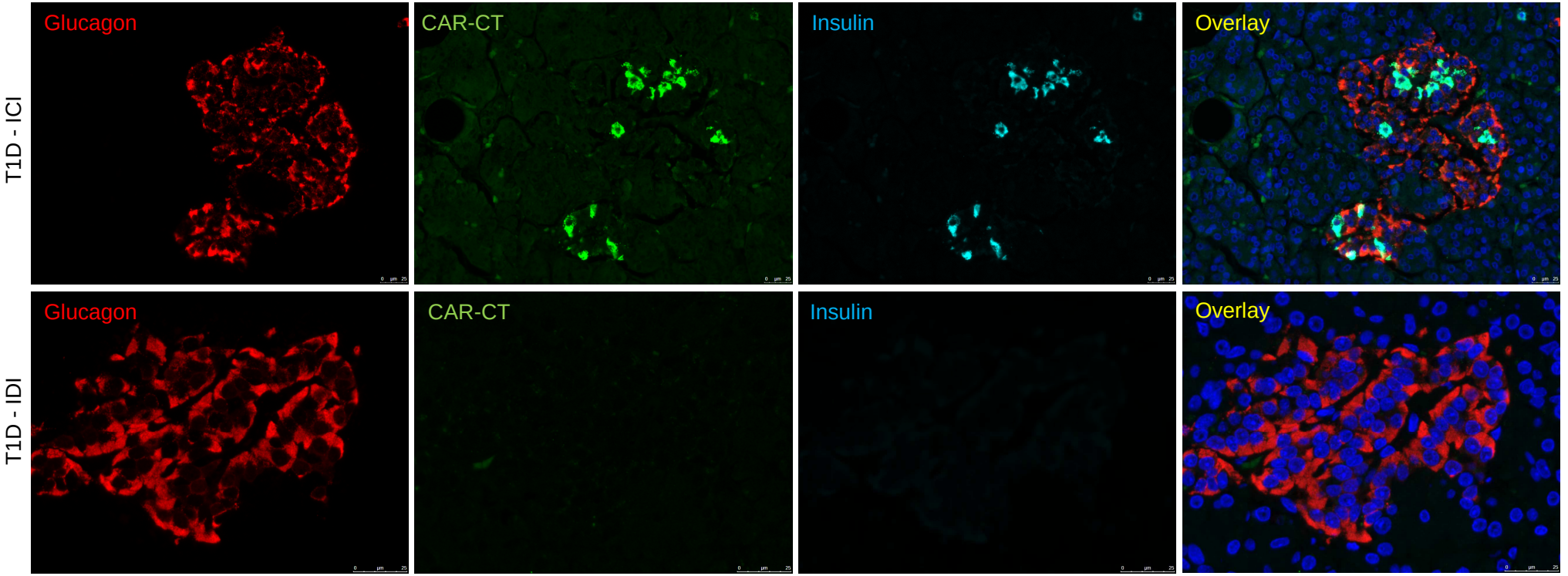

ESM Fig 3: CAR-SIV expression is observed only in the insulin containing islets of individuals with Type 1 diabetes patients and not in insulin deficient islets. Representative immunofluorescence staining of the CAR-SIV isoform (CAR-CT antibody; green) insulin (light blue), glucagon (red) and DAPI (dark blue) in an insulin containing islet (ICI; upper panel) and insulin deficient islet (IDI; lower panel) of a donor with Type 1 diabetes. Scale bar 25µm. These results are representative of findings in the pancreas of 10 Type 1 diabetes donors (ESM Table 1). CAR-SIV is expressed in T1D donor islets but only in beta cells (upper panel). Once the beta cells have been destroyed CAR-SIV expression is lost (lower panel). CAR-SIV expression in beta cells from autoantibody positive non-diabetic donors did not differ from that seen in autoantibody negative donors without diabetes (data not shown).

a.

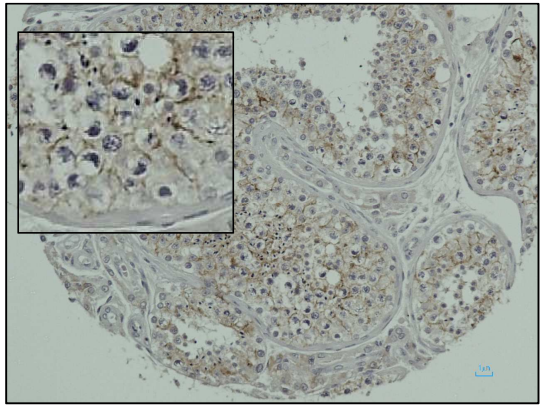

b.

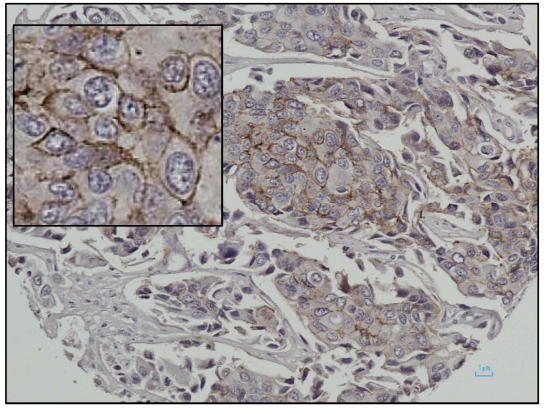

c.

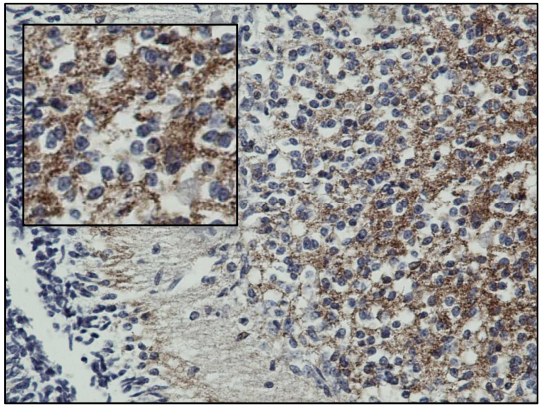

d.

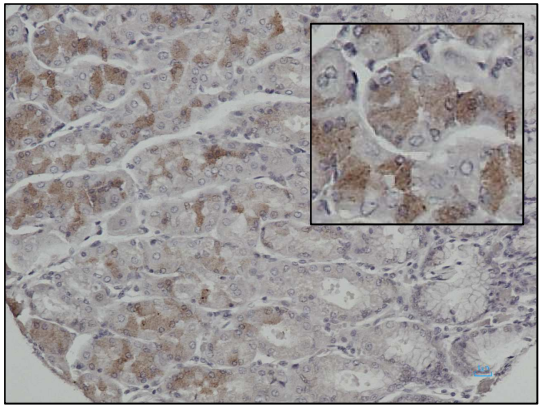

e.

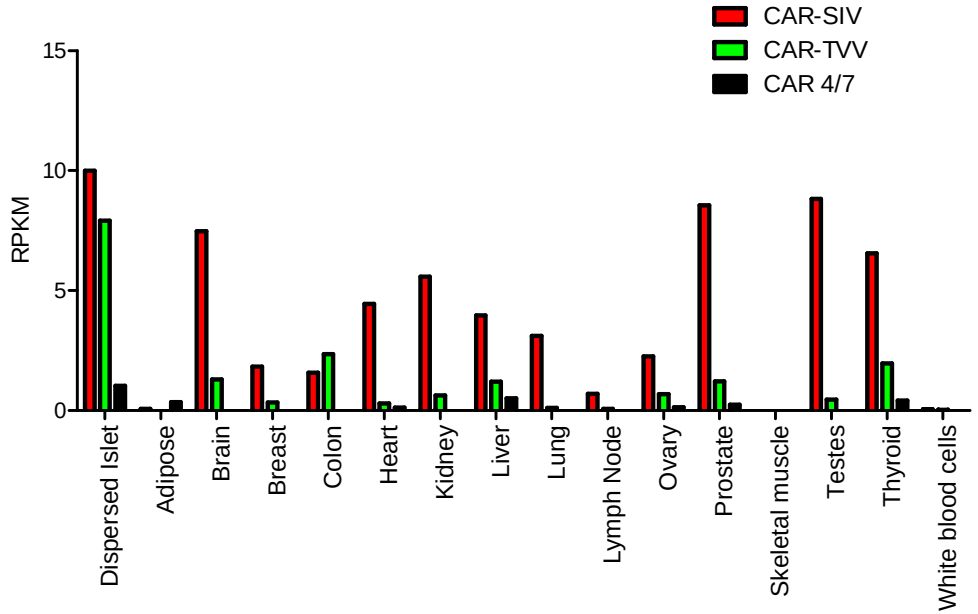

ESM Fig 4: CAR-SIV subcellular localisation and distribution in human tissue. Immunohistochemical staining demonstrating either surface membrane or granular distribution of CAR-SIV in different human tissues. **(a)** Testes, **(b)** Bladder small cell carcinoma, **(c)** Brain **(d)** Stomach. **(e)** RNA-seq analysis of *CXADR* isoforms supports the expression profile of CAR-SIV in dispersed human islets and various other normal human tissues. CAR-SIV is highly expressed in dispersed islets, brain, kidney, heart, prostate, testis and thyroid when compared to CAR-TVV and CAR 4/7.

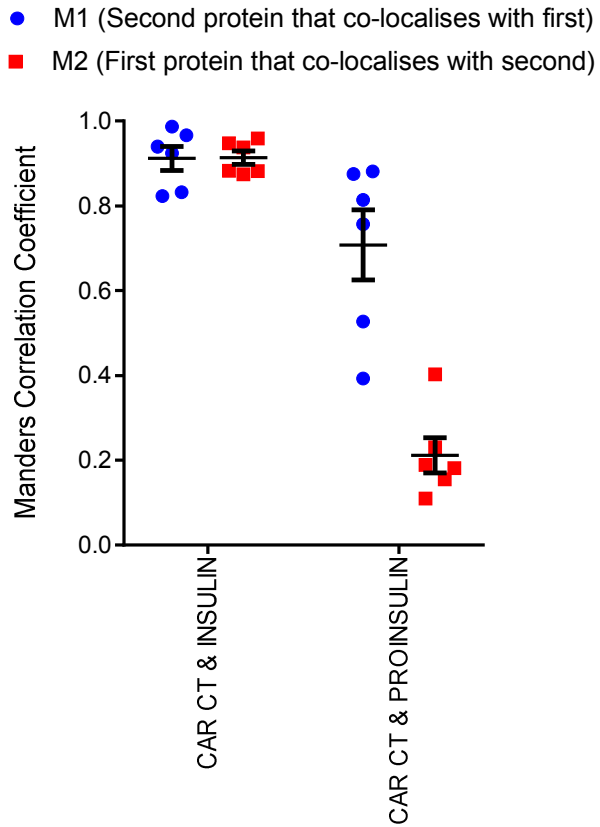

ESM Fig. 5 Manders Colocalisation Coefficient (MCC) analysis. This analysis allows us to assess how much of the proinsulin or insulin immunostaining is coincident with CAR-SIV and vice versa. This more detailed analysis has shown that the vast majority of CAR-SIV co-localises with insulin (MCC: 0.914±0.016) and that the same is also true for insulin co-localising with CAR-SIV (MCC: 0.912±0.028). This is consistent with them both being present in mature insulin secretory granules. In contrast, CAR-SIV does not co-localise to the same extent with proinsulin (MCC: 0.211±0.042), presumably because the majority of CAR-SIV is in the mature granules (which is supported by the immuno-EM quantitative analysis). In contrast, a higher proportion of proinsulin co-localises with CAR-SIV (MCC: 0.708±0.082) and this is likely to represent both CAR-SIV and pro-insulin in the immature granules as these emerge from the trans-Golgi.

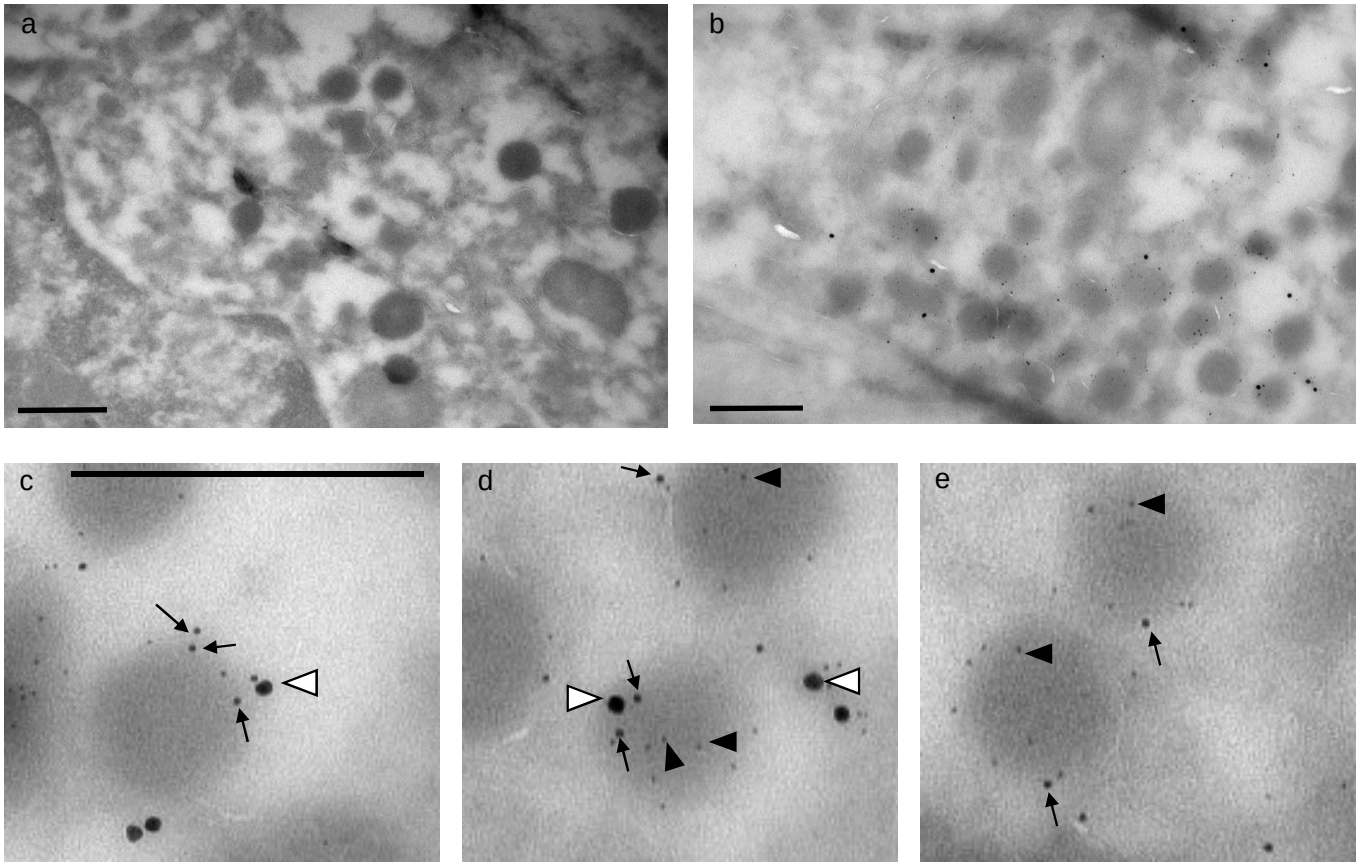

ESM Fig. 6 Cryo-immune EM analysis of insulin granules at different stages of maturation. Low magnification image (a) demonstrates no labelling of the pancreatic tissue when exposed to unconjugated gold particles and bridging antibodies. (b-e) Immunogold labelling of insulin (5nm gold; black triangle); CAR-SIV (10nm gold; black arrow) and proinsulin (20nm gold; white triangle) in thin frozen sections of human pancreas tissue. The higher magnification images reveal (c) immature granules positive for proinsulin and CAR-SIV, (d) maturing granules positive for proinsulin, insulin and CAR-SIV and (e) mature granules positive for insulin and CAR-SIV. Scale bar: 500 nm

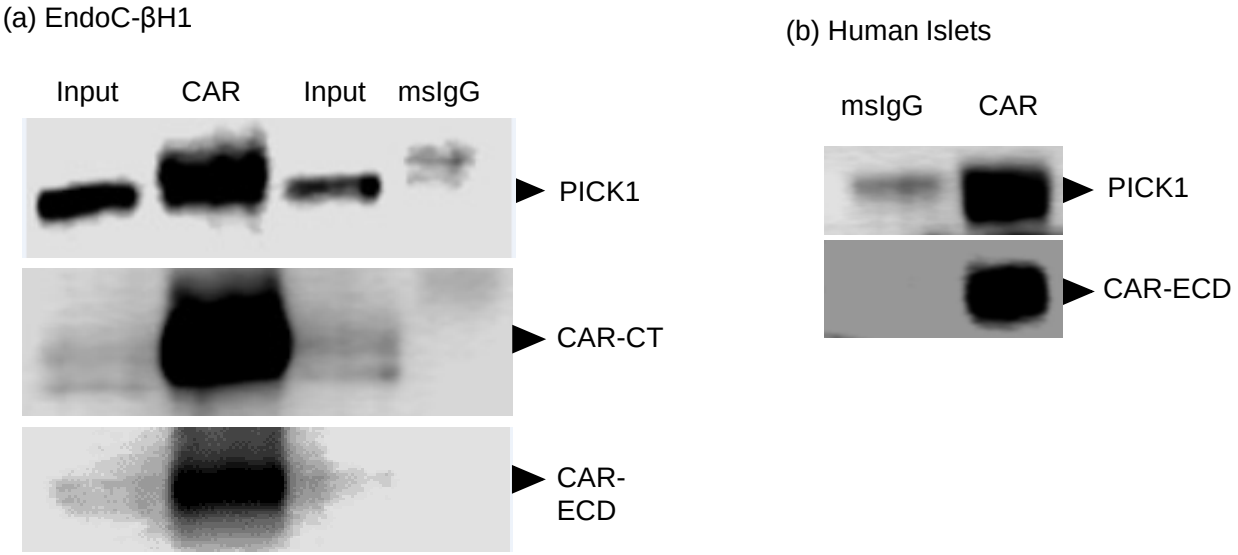

ESM Fig. 7 Immunoprecipitation of CAR from (a) EndoC-βH1 cells and (b) human islets also pulls down PICK1. Co-immunoprecipitation (see ESM Materials) was carried out with anti-CAR RmcB or anti-Mouse IgG (msIgG) as negative control. Immunoprecipitated proteins were analysed on Western blots probed with anti-PICK1. The membrane was then stripped and re-probed with anti-CAR CT or anti-CAR ECD. Input control (2%) was included as shown.